Comparative Supramolecular Chemistry of Coronene, Hexahelicene, and [18]Crown-6: Hydrated and Solvated Molecular Complexes of [18]Crown-6 with 5-Hydroxyisophthalic Acid and Related Di- and Tricarboxylic Acids**

Otto Ermer* and Jörg Neudörfl[a]

Abstract: The outer rim of C–H bonds of coronene (COR) and hexahelicene (HEL) is similar to that of the crown conformation of [18]crown-6 (CRO), which is exploited for crystal engineering of molecular complexes of CRO. However, although CRO does form the adduct $(TMA)_2 \cdot CRO \cdot (H_2O)_2$ (TMA = trimesic acid = 1,3,5-benzenetricarboxylic acid), its structure does not correspond to the H-bonded, three-connected honeycomb sheet architectures of $(TMA)_2 \cdot COR$ and $(TMA)_2 \cdot HEL$. Instead, porous, but noninterpenetrating, H-bonded four-connected sheets are observed, with the dihydrated, crown-shaped CRO molecules functioning as spacers rather than molecular guests. In the adduct $(CHTA)_2 \cdot CRO \cdot (H_2O)_5$ (CHTA = *cis*,*cis*-1,3,5-cyclohexanetricarboxylic acid), the tetrahydrated CRO molecules again take up the crown conformation and act as spacers, this time within porous, noninterpenetrating H-bonded three-connected sheets. The engineering goal of CRO-filled H-bonded, hexagonal honeycomb cavities similar to the COR- and HEL-filled TMA honeycomb pores in $(TMA)_2 \cdot COR$ and $(TMA)_2 \cdot HEL$ was met in the adduct $(HIPA)_6 \cdot CRO \cdot (H_2O)_{10}$ (HIPA = 5-hydroxyisophthalic acid), crystallized from aqueous EtOH. The crystal structure of this complex is on the one hand built up of isolated hexagonal honeycomb cavities established by six HIPA molecules cyclically linked through pairwise intercarboxylic H bonds. These cavities accommodate the crown-shaped CRO molecules, oriented such that maximally straight C–H···O contacts are enabled between its 12 equatorial H atoms and the surrounding 12 carboxylic groups of HIPA, in complete analogy to the situation prevailing in $(TMA)_2 \cdot HEL$ and (probably) $(TMA)_2 \cdot COR$. The second building block of $(HIPA)_6 \cdot CRO \cdot (H_2O)_{10}$ is represented by a centrosymmetric decameric water cluster, which has the connectivity of the carbon skeleton of a bishomocubane with opposite methylene bridges, in agreement with vibrational spectroscopic evidence on gaseous $(H_2O)_{10}$. The crystal architecture of the adduct as a whole may either be likened to a severely distorted NaCl-type lattice, with the $(HIPA)_6 \cdot CRO$ units replacing, for example, the Na^+ ions, and the water clusters substituting the Cl^- ions, or else to a system of stacked host sheets set up by C–H···O bonded $(HIPA)_6$ macrorings, which give rise to perpendicular channels taking up guest columns of alternating, H-bonded CRO and $(H_2O)_{10}$ units. Crystals of another, solvated HIPA–CRO adduct of the composition $(HIPA)_4 \cdot CRO \cdot (EtOH)_2$ were obtained from aqueous EtOH. Their crystal structure is related to those of $(TMA)_2 \cdot HEL$ and $(TMA)_2 \cdot COR$ inasmuch distorted HIPA honeycomb sheets are adopted, which may be developed from the hexagonal TMA sheets by replacing one third of the pairwise intercarboxylic linkages by single interphenolic H bonds. The cavities in the HIPA sheets are thus smaller than those of the TMA honeycomb sheets and elliptically shaped. The HIPA sheets associate in pairs yielding twin cavities which take up one CRO and two EtOH molecules. The CRO molecules are suspended in the twin HIPA cages through H bonds extended from the phenolic OH groups and relayed by interposed EtOH "bridges". In keeping with the elliptic shape of the pores in $(HIPA)_4 \cdot CRO \cdot (EtOH)_2$, the CRO molecules are not crown-shaped, but rather adopt the more rectangular form as observed in crystalline CRO itself. The crystal structure of a dihydrate of HIPA itself was analysed, too, which assembles in a complex three-dimensional H-bonded network. It is finally concluded that hydrated CRO appears to be an avid H-bond acceptor, in particular towards carboxylic acids functioning as H-bond donors.

Keywords: crown compounds · crystal engineering · hydrogen bonds · supramolecular chemistry · water decamer

Introduction

The prominent aromatic hydrocarbons coronene (COR), [18]annulene (ANN), and hexahelicene (HEL) have similar molecular shapes and chemically corresponding outer rims (Figure 1). It was shown in a previous communication[1] that COR and (racemic) HEL form molecular complexes with trimesic acid (TMA) since they fit well into the hexagonal chambers of the H-bonded TMA honeycomb sheets. These

[a] Prof. Dr. O. Ermer, J. Neudörfl
Institut für Organische Chemie der Universität
Greinstrasse 4, 50939 Köln (Germany)
Fax: (+49) 221-4705057

[**] Abbreviations of substances: CRO: [18]crown-6; COR: coronene; HEL: hexahelicene; ANN: [18]annulene; CR15: [15]crown-5; HIPA: 5-hydroxyisophthalic acid; TMA: trimesic acid (1,3,5-benzenetricarboxylic acid); CHTA: *cis*,*cis*-1,3,5-cyclohexanetricarboxylic acid; NIPA: 5-nitroisophthalic acid; IPA: isophthalic acid; DMGA: 2,2-dimethylglutaric acid; TGA: *trans*-glutaconic acid; GA: glutaric acid; HQ: hydroquinone.

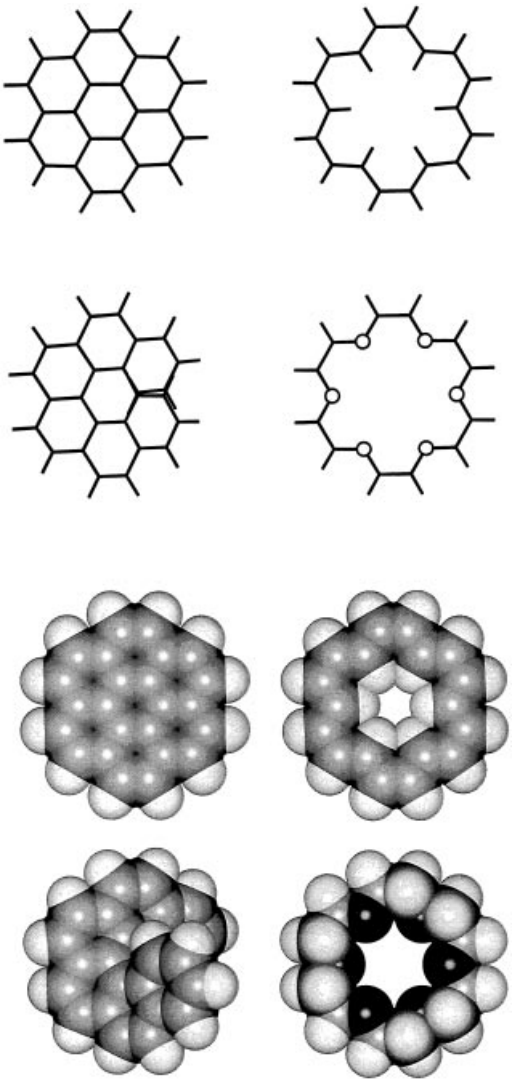

Figure 1. Stereochemical connection of COR, ANN, HEL, and the crown conformation of CRO. Top: line drawings; below: space-filling representations. Note the chemically and dimensionally similar outer rims of the molecules, which are drawn to the same scale.

complexes have the composition $(TMA)_2 \cdot COR$ and $(TMA)_2 \cdot HEL$ with the hydrocarbon guest molecules suspended in the host cavities by means of favorable C–H···O contacts. Here we extend this study to the prototypal crown ether molecule [18]crown-6 (CRO) the crown conformation of which exhibits a periphery dimensionally and chemically similar to that of COR, ANN, and HEL. More specifically, this refers to the 12 equatorial H atoms and C–H bonds of the crown conformation of CRO, which are sterically and directionally similar to the outer H atoms of the three circularly shaped aromatic hydrocarbons COR, ANN, and HEL (Figure 1; note also the common origin of the substance names "*coron*ene" and "*crown* ether"). These stereochemical interrelations are entirely analogous to those between the six equatorial H atoms of the chair form of cyclohexane and the hydrogen periphery of benzene, since the axial–equatorial differentiation of the H atoms of the chair form of cyclohexane can be transposed exactly to the crown form of CRO. This is illustrated in Figure 2, which shows that ideally the

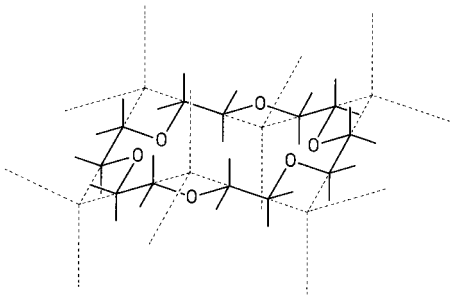

Figure 2. Conformational interrelation of the crown conformation of CRO and the chair form of cyclohexane (idealized). The directionalities of all bonds of both structures correspond to the space diagonals of one common cube. Note the fully analogous axial–equatorial differentiation of the C–H bonds in both conformations.

crown conformation of CRO of symmetry D_{3d} may be inscribed into a cyclohexane chair scaled up to approximately triple size, such that all C–C, C–O, and C–H bonds are directed parallel to the space diagonals of one common cube. Thus the ring torsion angles around the C–C bonds in the idealized crown conformation of CRO assume the magnitude 60° with the signs alternating, while those around the C–O bonds are antiplanar (180°).

It appears that our comparative supramolecular planning would require the crown form of CRO to be the most favorable conformation, but very probably this is not the case.[2] While almost free from torsional and angle strain, this form suffers from severe nonbonded repulsions between the oxygen atoms, all directed towards the interior of the ring including in particular their equatorial lone pairs. However, if these repulsions are alleviated through complexation of metal cations or through hydrogen bonding with suitable partners, the crown conformation of CRO is turned into the energetical favorite, as has been frequently observed.[2b] In the present context, we accordingly surmised that specifically hydration might come to our aid in stabilizing the crown conformation. This indeed did occur as reported herein. In relating COR and CRO as supramolecular congeners, the energetic aspect regarding the strength of the C–H···O contacts both molecules are capable of establishing, is evidently also of relevance. Because of the carbon sp^2 hybridization in COR, its H atoms are more acidic than those of CRO involving sp^3 C atoms. Therefore, COR should be a better H donor for C–H···O bonding than CRO although some H activation is provided in the cyclic hexaether, too, by the electronegative O atoms bonded to the methylene groups. CRO may thus also be expected to exhibit a reasonable inclination towards engagement in C–H···O contacts of appreciable strength. Our supramolecular experiments with CRO were initially targeted to uncover additional support as regards the orientation of the COR molecules in the TMA host chambers of $(TMA)_2 \cdot COR$ the structure of which could not be fully solved by crystallographic means, probably due to stacking disorder of the honeycomb sheets.[1] Eventually, however, the work took a rather different course beyond the initial goal, and was rewarded by some unexpected and intriguing observations, which we deem worth reporting.

0947-6539/01/0722-4962 $ 17.50+.50/0 *Chem. Eur. J.* **2001**, *7*, No. 22

Results and Discussion

Hydrated CRO functioning as spacer in the molecular complexes with TMA, CHTA, DMGA, and TGA: Quite naturally, the creation of a molecular complex of TMA and CRO was attempted first. Indeed good parallelepipedic crystals of a 2:1 adduct were readily obtained in the form of a dihydrate from aqueous ethanol, corresponding to the formulation $(TMA)_2 \cdot CRO \cdot (H_2O)_2$. Although the 2:1 molar ratio of TMA and CRO would comply with a honeycomb sheet architecture as in $(TMA)_2 \cdot COR$ and $(TMA)_2 \cdot HEL$,[1] the X-ray analysis furnished an entirely different crystal structure of $(TMA)_2 \cdot CRO \cdot (H_2O)_2$. A section of the triclinic crystal architecture (space group $P\bar{1}$ with one formula unit in the cell; see Table 1) is shown in Figure 3a. The centrosymmetric CRO molecule takes up the crown conformation and is doubly hydrated through four hydrogen bonds engaging the water H atoms (O···O separations 2.842(2) and 2.899(2) Å). The water molecules are involved in a third H bond the H atom of which is donated by a carboxyl group of a TMA molecule (O···O 2.538(2) Å). In turn, the TMA molecules are grouped in macrocyclic, centrosymmetric dimers brought about by two opposite single intercarboxylic H bonds (O···O 2.710(1) Å). The remaining carboxyl group of the TMA molecules is utilized for linking up the macrocyclic dimers through the usual centrosymmetric H bond pairs to form straight chains (O···O 2.627(1) Å). These chains of doubly H-bonded macrocyclic TMA dimers are coupled by the hydrated CRO molecules through the above-mentioned H bonding pattern, such that ultimately two-dimensional four-connected sheets are seen to emerge, which are essentially planar. Figure 3b gives an impression of these extended supramolecular sheet architectures. The dihydrated CRO molecules may be viewed as spacers separating the TMA chains and thus giving rise to roughly parallelogram-shaped cavities, into which CRO molecules of neighboring, non-interpenetrating sheets extend (Figure 3c).

CRO was found to also form a hydrated complex with 5-nitroisophthalic acid (NIPA) of the composition $(NIPA)_2 \cdot CRO \cdot (H_2O)_2$ the crystal structure of which we investigated as well. The essential X-ray data of these crystals with the same molar component ratios as in the above TMA complex, are as follows: triclinic, space group $P\bar{1}$, $Z = 1$; $a = 7.6149(2)$, $b = 8.0229(2)$, $c = 14.8850(4)$ Å, $\alpha = 104.195(2)$, $\beta = 104.666(1)$, $\gamma = 92.117(2)^\circ$, $V = 848.12$ Å^3; $R1 = 0.054$, 3043 significant reflections. The cell dimensions are closely similar to those of $(TMA)_2 \cdot CRO \cdot (H_2O)_2$ (see Table 1), and the structure analysis revealed the detailed crystal architectures of both adducts to be entirely analogous as well. The structure of $(NIPA)_2 \cdot CRO \cdot (H_2O)_2$ may be developed out of that of $(TMA)_2 \cdot CRO \cdot (H_2O)_2$ essentially through rupture of the H bonds holding the macrocyclic TMA dimers together and replacement of the affected carboxyl groups, which are not H-bonded to the hydrated CRO molecules, by nitro functions. Rather than by sheets, the crystal structure of the NIPA complex is thus instead characterized by H-bonded chains with alternating hydrated CRO molecules and doubly connected NIPA pairs. We could furthermore create a hydrated complex of TMA with [15]-crown-5 (CR15) with the composition $(TMA)_2 \cdot CR15 \cdot (H_2O)_2$. The crystal structure of this adduct is fully analogous to that of $(TMA)_2 \cdot CRO \cdot (H_2O)_2$ with practically the same H-bonded four-connected sheets. This is also reflected in the similar cell data, but it is pointed out that the CR15 molecules, which occupy centrosymmetric sites, are necessarily disordered. The basic X-ray results of $(TMA)_2 \cdot CR15 \cdot (H_2O)_2$ are the following: triclinic, space group $P\bar{1}$, $Z = 2$; $a = 7.2649(2)$, $b = 15.2815(3)$, $c = 15.7108(4)$ Å, $\alpha = 112.312(1)$, $\beta = 92.966(1)$, $\gamma = 91.254(2)^\circ$, $V = 1609.81$ Å^3; $R1 = 0.109$, 5203 significant reflections. The cell dimensions may be compared with those of $(TMA)_2 \cdot$

Table 1. Crystal and refinement data.[a]

Complex	$(HIPA)_6 \cdot CRO \cdot (H_2O)_{10}$		$(HIPA)_4 \cdot CRO \cdot (EtOH)_2$	$(TMA)_2 \cdot CRO \cdot (H_2O)_2$	$(CHTA)_2 \cdot CRO \cdot (H_2O)_5$	$HIPA \cdot (H_2O)_2$
crystal system	triclinic		triclinic	triclinic	triclinic	monoclinic
space group	$P\bar{1}$		$P\bar{1}$	$P\bar{1}$	$P\bar{1}$	$P2_1/c$
Z	1		1	1	1	4
T [K]	298	100	298	298	298	298
a [Å]	10.2371(3)	10.0250(2)	8.7000(3)	7.4985(2)	7.5261(2)	3.6740(1)
b [Å]	14.5422(5)	14.4561(3)	13.0465(4)	8.0224(2)	11.4106(3)	24.9929(7)
c [Å]	14.3422(4)	14.3362(2)	13.0463(4)	14.7148(3)	12.8701(3)	10.2409(3)
α [°]	115.498(1)	115.422(1)	119.662(2)	77.046(1)	94.606(2)	
β [°]	99.725(1)	100.337(1)	89.848(2)	79.484(1)	103.192(1)	99.443(2)
γ [°]	103.801(1)	103.019(1)	97.100(2)	84.412(1)	111.097(2)	
V [Å^3]	1779.41	1735.87	1273.96	846.69	987.78	927.62
d_x [g cm^{-3}]	1.435	1.471	1.414	1.413	1.323	1.562
d_m [g cm^{-3}]	1.43	–	–	–	–	–
N_{tot}	14973	29162	8606	13321	10134	9087
N_{indep}	7708	11984	5463	3701	4256	2684
N_{sig}	5662	10581	4220	3083	3216	2369
ρ_{res} [e Å^{-3}]	0.29	0.54	0.25	0.27	0.45	0.37
R_{int}	0.022	0.016	0.021	0.014	0.013	0.020
$R1$	0.044	0.035	0.050	0.045	0.057	0.039
$wR2$	0.126	0.104	0.143	0.128	0.169	0.109

[a] The macroscopic density d_m of $(HIPA)_6 \cdot CRO \cdot (H_2O)_{10}$ was measured by flotation in CCl_4/mesitylene. N_{tot}, total number of reflections recorded; N_{indep}, total number of independent reflections; N_{sig}, total number of significant independent reflections with $F > 4\sigma(F)$; ρ_{res}, maximum residual electron density; R_{int}, agreement index among intensities of equivalent reflections. $R1$ and $wR2$ indices include N_{sig} and N_{indep} reflections, respectively.

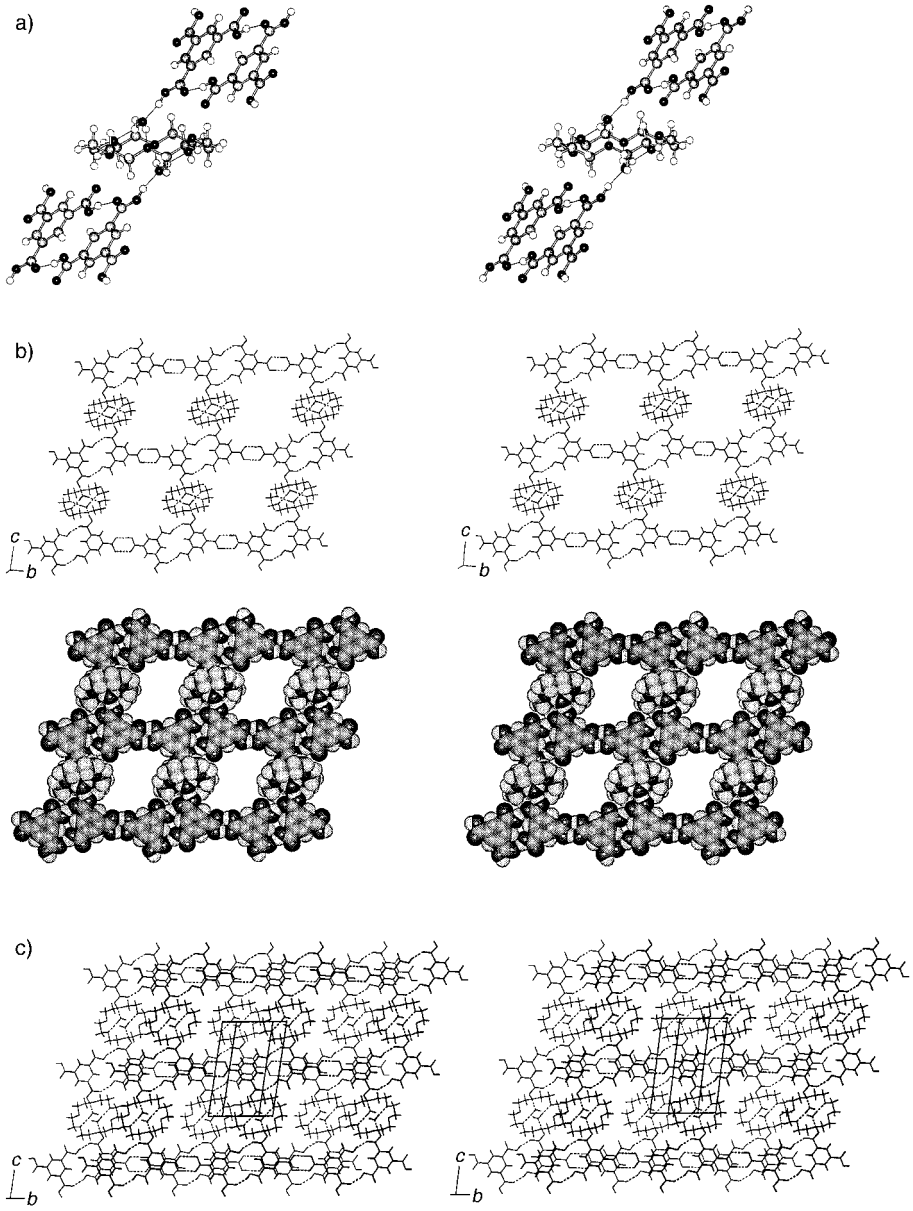

Figure 3. Crystal structure of $(TMA)_2 \cdot CRO \cdot (H_2O)_2$. a) Stereoview of a dihydrated CRO spacer molecule H-bonded by two TMA molecules. b) Line and space-filling stereodrawings of a section of a single porous, four-connected planar sheet. c) Stereo line drawing of two neighboring noninterpenetrating sheets (top layer in heavy line). The voids of the porous layers are filled by the voluminous CRO spacers of neighboring sheets.

$CRO \cdot (H_2O)_2$ (Table 1) and $(NIPA)_2 \cdot CRO \cdot (H_2O)_2$, but in doing so it should be noted that the cell of the CR15 complex is roughly doubled since it holds twice the number of molecules.

Why do the TMA molecules in the crystals of $(TMA)_2 \cdot CRO \cdot (H_2O)_2$ not join to form honeycomb sheets with the (hydrated) CRO molecules embedded in the hexagonal cavities? In other words: Why is the structure of this complex so different from that of the adducts $(TMA)_2 \cdot COR$ and $(TMA)_2 \cdot HEL$, which do build up hydrocarbon-loaded honeycomb sheets? A relevant reason is probably to be sought in the fact that the thickness of the disc-shaped (hydrated) crown conformation of CRO is substantially larger than that of the TMA molecule, that is about 4.5 versus 3.3 Å. This incompatibility of molecular thicknesses might preclude effective sheet stacking. We therefore thought that replacing TMA by *cis*,*cis*-1,3,5-cyclohexanetricarboxylic acid (CHTA) with similarly disposed carboxylic groups might be more promising in order to encourage the formation of the targeted supramolecular honeycomb sheets. The cyclohexane chair conformation of CHTA and the crown conformation of CRO practically have the same thickness, which follows from the geometrical interrelations of both conformations as pointed out in the Introduction and highlighted in Figure 2. Of course, the equatorial carboxylic groups of CHTA are not entirely coplanar as in TMA, and they are still comparatively "thin", which might weaken the design concept. Experiment had to decide, of course, and supplied us with the factual answers as reported in the following. Good crystals could again be easily grown from a 2:1 solution of CHTA and CRO in aqueous ethanol, this time with the composition $(CHTA)_2 \cdot CRO \cdot (H_2O)_5$.

X-ray analysis showed CRO to be tetrahydrated and to take up the crown conformation. This molecular ensemble occupies a crystallographic center of symmetry (space group $P\bar{1}$ with one formula unit in the cell; see Table 1). The fifth water molecule is positionally disordered and may be referred to as "interstitial", in a sense pointed out further below.

The structure of the tetrahydrated CRO molecule may be derived from that of the dihydrate as occurring in $(TMA)_2 \cdot CRO \cdot (H_2O)_2$ by insertion of two additional water molecules such that all six oxygen atoms of CRO become involved in H bonding. The tetrahydrate is held together by a total of eight H bonds, two of which link water molecules; the $O \cdots O$ distances of the latter H bonds measure 2.674(2) Å, while the others range from 2.853(2) to 2.880(2) Å. This H bonding pattern is illustrated in Figure 4a, which should be compared to Figure 3a in order to appreciate the interrelations with the CRO dihydrate of the TMA complex. The structure of the present tetrahydrate of CRO closely corresponds to that previously encountered in the hydrated complex of phos-

0947-6539/01/0722-4964 $ 17.50+.50/0 *Chem. Eur. J.* **2001**, *7*, No. 22

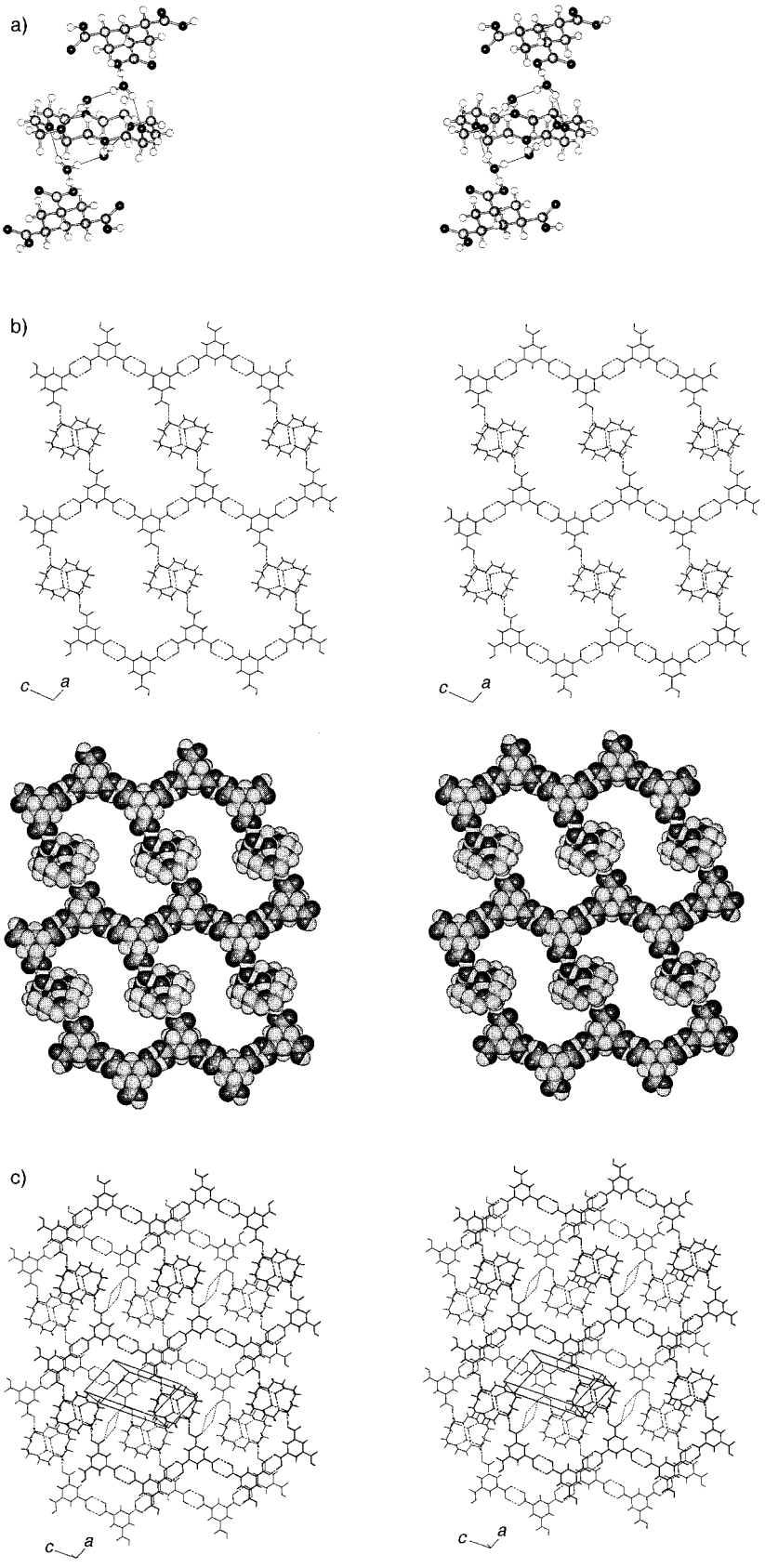

Figure 4. Crystal structure of $(CHTA)_2 \cdot CRO \cdot (H_2O)_5$. The representations correspond to those of Figure 3. a) Tetrahydrated CRO molecule H-bonded by two CHTA molecules. b) Section of a single porous, three-connected puckered and distorted honeycomb sheet. c) Two neighboring porous sheets; filling of voids by CRO spacers of neighboring layers. The position and H-bond connectivities of the disordered, interstitial water molecules are indicated (dashed "lozenges").

phoric acid and CRO of the composition $(H_3PO_4)_2 \cdot CRO \cdot (H_2O)_6$.[3]

The CHTA molecules of $(CHTA)_2 \cdot CRO \cdot (H_2O)_5$ form zigzag chains in the crystal held together by standard pairwise intercarboxylic H bonds across centers of symmetry ($O \cdots O$ distances 2.649(2) and 2.635(2) Å). The remaining third carboxylic groups of CHTA not engaged in the zigzag chains donate their H atoms to H bonds directed towards the O atom of a water molecule of the CRO tetrahydrate ensembles ($O \cdots O$ distance 2.595(2) Å), that is one of those water molecules not present in the CRO dihydrate of $(TMA)_2 \cdot CRO \cdot (H_2O)_2$ (Figure 4a). Thus we finally end up with CHTA zigzag chains linked by $CRO \cdot (H_2O)_4$ spacers through these single carboxyl–water H bonds producing distorted (oblique, elongated), puckered honeycomb sheets as illustrated in Figure 4b. These three-connected sheets are highly porous, but they do not interpenetrate and have their cavities filled by CRO molecules of neighboring sheets (Figure 4c). The cavities in the sheets of $(CHTA)_2 \cdot CRO \cdot (H_2O)_5$ are larger than those of $(TMA)_2 \cdot CRO \cdot (H_2O)_2$ and roughly take the shape of the shell of a peanut, that is they are equipped with a waist. Filling-up these pores requires the involvement of two CRO molecules extending into them from two neighboring sheets above and below. The space-filling structural mechanism in $(TMA)_2 \cdot CRO \cdot (H_2O)_2$ is similar (Figure 4c and Figure 3c). So, in conclusion, we note that by combining CHTA and (hydrated) CRO we indeed managed to engineer porous honeycomb sheets, although admittedly only partially of the kind we were actually aiming at. Rather than playing the role of guest molecules within the targeted CHTA honeycomb

sheets held together exclusively by pairwise intercarboxylic H bonds, the CRO molecules choose to break up and become inserted into one third of these intercarboxylic linkages. In doing so, the CRO molecules call upon the assistance of four water molecules and altogether give rise to a sheet fabric characterized by elongated, oblique honeycomb chambers. The CHTA molecules of the sheets are not entirely coplanar but rather assume a (relatively shallow) super-chairlike puckered arrangement (Figure 4b) analogous to the carbon atoms of a sheet of *trans*-fused six-membered chair rings in diamond. In a difference electron density map of the CHTA complex a residual peak showed up, which was only 0.82 Å away from a center of symmetry. It was interpreted as a positionally disordered , interstitial water molecule, and accordingly refined with half occupancy. Thus the formulation of the adduct as altogether a pentahydrate, that is $(CHTA)_2 \cdot CRO \cdot (H_2O)_5$, becomes clear. The hydrogen atoms of the disordered fifth water molecule could, however, not be located, in contrast to those of the four water molecules H-bonded to CRO. Closer inspection of the crystal structure suggests that the disordered water molecule is H-bonded to two carbonyl O atoms of carboxyl groups belonging to two centrosymmetrically related CHTA molecules of different, neighboring honeycomb sheets (O···O distances 2.95(1) and 2.97(1) Å, respectively); hence its characterization as interstitial water sitting between two sheets. The water-bridged carboxy groups have their hydroxy groups H-bonded to the $CRO \cdot (H_2O)_4$ spacer moieties. Including the interstitial water, the H-bonded network of $(CHTA)_2 \cdot CRO \cdot (H_2O)_5$ is altogether three-dimensional (Figure 4c).

We finally see that through replacing TMA by CHTA as a supramolecular partner of (hydrated) CRO we indeed got a step closer to the desired honeycomb sheets, but did in fact not reach our engineering goal of having a CRO molecule embraced by a ring of six tricarboxylic acid molecules held together by pairwise intercarboxylic H bonds. Next we focussed on a possible 6:1 molecular complex of isophthalic acid (IPA) with "insulated" CRO-carrying hexagonal honeycomb cages held together by six pairs of intercarboxylic H bonds in exactly the same way as TMA is capable of forming sheets of fused honeycomb cavities. The supramolecular relationship is evident since IPA is a substructure of TMA with the required *meta*-positioned carboxylic groups. Attempts to cocrystallize IPA and CRO from ethanol (6:1 molar ratio) did not, however, produce any evidence in support of molecular complex formation. A reason for this supramolecular recalcitrance of IPA might possibly lie in its own crystal structure, which, judging from the high melting point of 348 °C, appears to be particularly favorable and may thus not be expected to be given up readily. In their crystals, the IPA molecules are joined pairwise by intercarboxylic H bonds to form planar zigzag chains.[4] Similar to the pair TMA/CHTA, *cis*-1,3-cyclohexanedicarboxylic acid was also subjected to crystallizations in the presence of CRO (ethanol, 6:1 molar ratio), but again to little avail, that is no crystals of a 6:1 complex could be obtained. The same holds for a number of further 5-substituted IPA systems (in addition to NIPA; see above), which were also combined with CRO in various crystallization experiments. Another rather obvious dicarboxylic acid candidate for a 6:1 molecular honeycomb complex with CRO would be glutaric acid (GA) given its W-shaped carbon backbone. However, cocrystallizations of GA and CRO from ethanol (6:1 molar ratio) did not furnish evidence in support of complex formation. On the other hand, similar experiments with 2,2-dimethylglutaric acid (DMGA) produced crystals of a 2:1 complex of DMGA with dihydrated CRO, corresponding to the composition $(DMGA)_2 \cdot CRO \cdot (H_2O)_2$. X-ray analysis gave the following essential crystallographic data: monoclinic, space group $P2_1/c$, $Z = 2$ formula units; $a = 13.5539(3)$, $b = 8.0371(2)$, $c = 15.0622(5)$ Å, $\beta = 90.836(2)^\circ$; $R1 = 0.047$, 3817 significant reflections. The CRO molecules take up the crown conformation and are dihydrated in the same fashion as reported above for $(TMA)_2 \cdot CRO \cdot (H_2O)_2$. The DMGA carbon backbone is not W-shaped which, quite apart from the stoichiometry, rules out the formation of a honeycomb-type complex. Instead, the DMGA molecules form singly H-bonded chains with carboxyl OH groups sticking out laterally. Each two of the chains are H-bonded through these lateral OH groups to dihydrated CRO molecules to form ribbons with a ladder-type connectivity; Figure 5a provides illuminating illustrations. Lastly, *trans*-glutaconic acid (TGA) was combined with CRO, and crystals of a monohydrated 1:1 complex of composition $TGA \cdot CRO \cdot H_2O$ were obtained from ethanol. The basic data of the ensuing X-ray analysis are: monoclinic, space group Cc, $Z = 4$ formula units; $a = 13.3234(4)$, $b = 9.9485(2)$, $c = 16.2155(4)$, $\beta = 92.947(1)^\circ$; $R1 = 0.057$, 2740 significant reflections. In these crystals the hydrated CRO molecules again take up the crown conformation, despite the H-binding of only a single water molecule. The TGA molecules are not W-shaped and bind to the $CRO \cdot H_2O$ moieties via single O(H)O hydrogen bonds towards the water O atoms. This results in singly H-bonded chains of alternating TGA and $CRO \cdot H_2O$ units, which may be appreciated by viewing Figure 5b. The structure may also be looked upon as consisting of singly H-bonded chains of alternating TGA and water molecules, with the carboxylic groups functioning as H-bond donors. Every water molecule of these chains donates its two H atoms to lateral, partially bifurcated H bonds towards ether O atoms of a CRO molecule. For clarity, it is noted finally that a 6:1 ratio of the diacids considered and CRO is not a strict prerequisite for the formation of CRO-filled insulated honeycomb cages in the crystal. In principle, both larger and smaller ratios would also allow this structural motif, but would in the first case require additional diacid molecules not involved in the macrocyclic hexameric aggregates, and in the second case additional CRO molecules exocyclic with respect to these large H-bonded hexagons housing already CRO endocyclically.

Structure of the molecular "honeycomb complex" $(HIPA)_6 \cdot CRO \cdot (H_2O)_{10}$ involving a decameric water cluster: Eventually attempts were made to grow crystals of a 6:1 complex of 5-hydroxyisophthalic acid (HIPA) and CRO. HIPA is relatively closely related to TMA being likewise equipped with three acid hydroxy groups, which are capable of donating their H atoms to good O(H)O hydrogen bonds. Formally, TMA may be turned into HIPA by decarbonylation. However, although the three acid functions of both HIPA and TMA are

  0947-6539/01/0722-4966 $ 17.50+.50/0 *Chem. Eur. J.* **2001**, *7*, No. 22

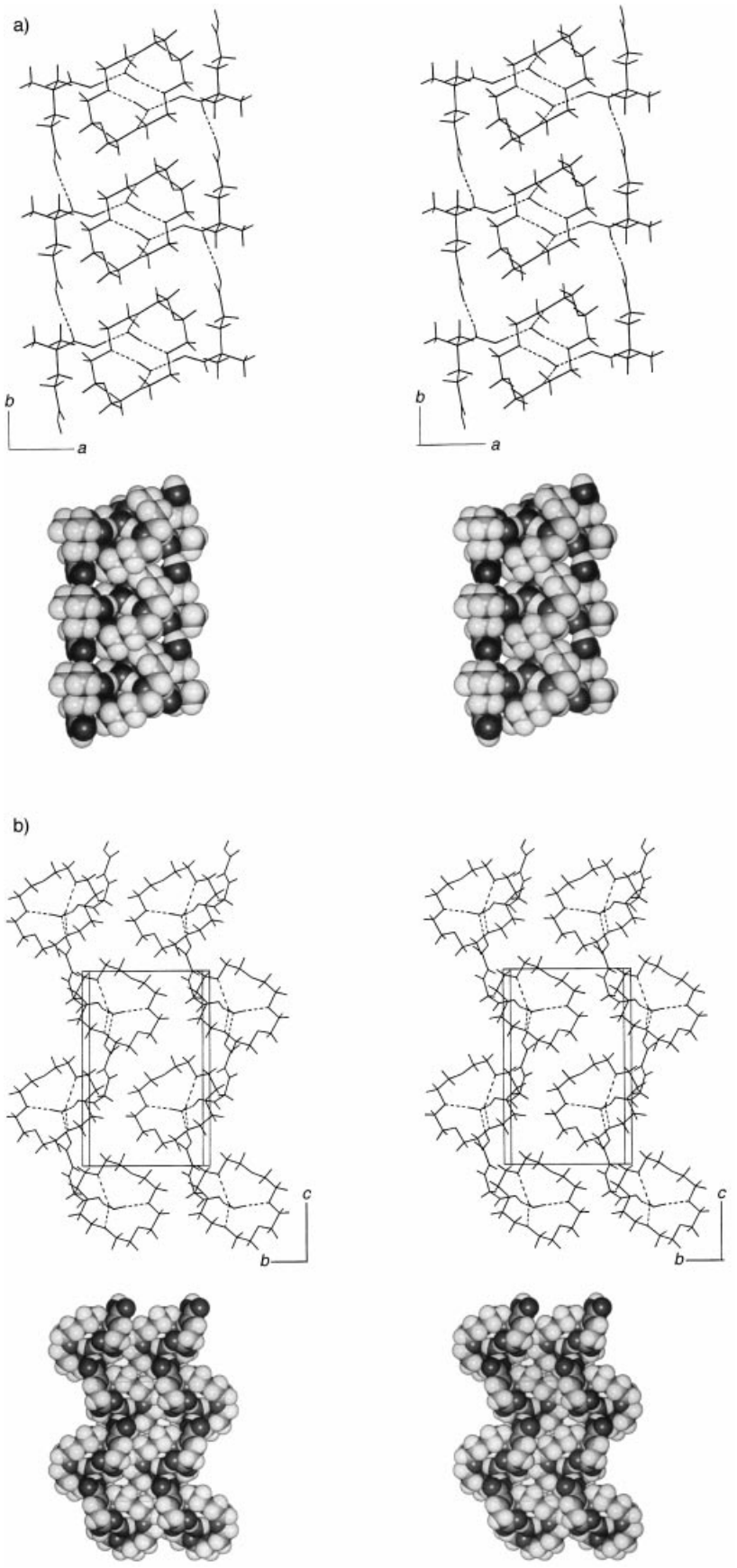

Figure 5. a) Crystal structure of $(DMGA)_2 \cdot CRO \cdot (H_2O)_2$. Stereo line and space-filling diagrams of a section of a ladder-type double chain of singly H-bonded DMGA molecules joined bydihydrated CRO spacers. b) Crystal structure of $TGA \cdot CRO \cdot H_2O$. A section of two neighboring chains of singly H-bonded, alternating TGA and $CRO \cdot H_2O$ units is shown.

coplanar and *meta*-positioned with respect to one another, the directionality of the three O–H bonds deviates in both molecules. In TMA, the O–H bonds are trigonally oriented and span angles of 120°, whereas in HIPA they are less symmetrically related spanning angles of 60, 120, and 180°. It is noted at this point that two ether derivatives of HIPA, that is 5-decyloxy- and 5-octyloxyisophthalic acid, were found previously to build up in the crystal the hexameric H-bonded honeycomb cages of interest in our present context.[5] However, the associated hexagonal cavities are not filled up by guest molecules in these cases but rather by the alkyl side chains of diacid molecules themselves assigned to neighboring hexameric aggregates in the crystal. By cocrystallizing HIPA and CRO the desired insulated hexagonal honeycomb cages made up of six cyclically H-bonded HIPA molecules could indeed be engineered, in the cavities of which the hydrated CRO molecules are anchored. The crystal structure of this host–guest compound involves in addition water molecules as a key architectural element and caught our enthusiasm with a number of fascinating and unexpected highlights, which are communicated in the following. From an ethanol solution of HIPA and CRO of molar ratio 6:1 large crystals were obtained under ambient (humid) conditions, which mostly took the shape of thick basalt-like rods of roughly hexagonal or rhomb-like cross-section and capped by approximately trigonal-pyramidal faces. The crystals may be rather smoothly cleaved perpendicular to their long axis and turned out stable for months without taking any special precautions. They proved to consist of a decahydrated 6:1 adduct of HIPA and CRO,

corresponding to the formulation $(HIPA)_6 \cdot CRO \cdot (H_2O)_{10}$. The space group of the triclinic crystals is $P\bar{1}$ with one formula unit in the cell, such that we are altogether faced with three crystallographically independent HIPA molecules, a centrosymmetric CRO molecule, and five independent water molecules (see Experimental Section and Table 1). To begin with, the X-ray reflection intensities were routinely measured at room temperature and subsequently at low temperature (100 K; Table 1). This was done to generally increase the precision of the measurement and, in particular, to study the temperature dependence of the hydrate achitecture, which had shown certain peculiarities in the room temperature experiment.

In the crystals of $(HIPA)_6 \cdot CRO \cdot (H_2O)_{10}$ the molecular constituents assemble to build up a three-dimensional network, which may conceptually best be penetrated by founding it on two particularly conspicuous building blocks. Expectedly, one is represented by the CRO-filled honeycomb cages as provided by six HIPA molecules cyclically linked by six standard intercarboxylic H bond pairs. The other consists of decameric water clusters held together by an array of 14 O(H)O hydrogen bonds. These building blocks are both centrosymmetric in the crystal. Figure 6 shows a section of the crystal structure with a pair each of the building blocks, together with the outlines of the unit cell. In the solid, the $(HIPA)_6 \cdot CRO$ and $(H_2O)_{10}$ units are three-dimensionally interlinked by further O(H)O hydrogen bonds engaging the phenolic OH groups of HIPA and the ether O atoms of CRO. We turn our attention first to the structures of the $(HIPA)_6 \cdot CRO$ and $(H_2O)_{10}$ building blocks themselves and subsequently consider their assembly in space.

CRO-Filled hexagonal H-bonded $(HIPA)_6$ honeycomb cages in $(HIPA)_6 \cdot CRO \cdot (H_2O)_{10}$: Within the $(HIPA)_6$ honeycomb cages the centrosymmetric CRO molecules assume the crown conformation (Figure 7) with approximate D_{3d} symmetry. However, significant deviations from the latter high symmetry are observed, which very probably have their origin in the mode of H bonding between CRO and the $(H_2O)_{10}$ clusters (see below). The O···O distances of the intercarboxylic H bond linkages between the HIPA molecules, which are obviously not related by crystallographic centers of symmetry, cover the rather narrow range from 2.579(1) to 2.608(1) Å with the normal average value of 2.597 Å (100 K). As envisaged, the CRO molecules are indeed suspended in the $(HIPA)_6$ cavities through C–H···O contacts between the 12 equatorial H atoms of CRO and the *endo*-macrocylic carboxyl O atoms of HIPA (Figure 7). The associated C···O distances range from 3.518(1) to 3.886(1) Å, average 3.696 Å, and the H···O distances (uncorrected) span values between 2.61(1) and 2.91(1) Å, average 2.75 Å. The respective C–H···O angles extend from 156(1) to 178(1)°, average 165° (all values measured at 100 K). The H···O distances may appear somewhat long, but this is due to the shortened C–H distances resulting (as usual) from the refinements (range 0.96(1)–0.98(1) Å, average 0.97 Å). If this C–H foreshortening of about 0.13 Å is taken into account, the H···O contacts in the honeycomb cages come close to the sum of the van der Waals radii of H and O. There are two symmetric possibilities to orient the CRO molecules in the $(HIPA)_6$ cavities, one with maximum straightness of the C–H···O interactions between CRO and HIPA, the other with markedly more bent C–H···O contacts. The two orientations are related by a rotation about 30° in the molecular mean plane of CRO. Figure 7a shows that, as expected, the CRO orientation enabling more straight C–H···O contacts is chosen. This corroborates our previous conclusions as regards the orientation of COR within the TMA honeycomb cavities of the molecular complex $(TMA)_2 \cdot COR$, and is fully analogous to the respective orientation of HEL in the adduct $(TMA)_2 \cdot HEL$.[1] It is parenthetically noted that the orientational problem of COR provided the original stimulus for the present work, since a direct solution by X-ray means had not been possible (see Introduction). A comparison of Figure 1 and Figure 2a in reference [1] with Figure 7a of the present work demonstrates rather impressively the apparently influential role of the C–H···O contacts for controlling the orientation of CRO, HEL, and (probably) COR in the honeycomb host cavities of HIPA and TMA, respectively. Clearly, the large number of 12 such contacts within a cavity matters, multiplying the rather small effect of a single weak C–H···O interaction. The average deviation from linearity of the C–H···O triads in the honeycomb cages of $(HIPA)_6 \cdot CRO \cdot (H_2O)_{10}$ amounts to 15°, as is evident from the above C–H···O angles. This deviation is more or less inevitable and is essentially a consequence of the quite obvious fact that the "equatorial" C–H bonds of the crown conformation of CRO are not entirely coplanar and do not run exactly perpendicular to the molecular S_6 axis.

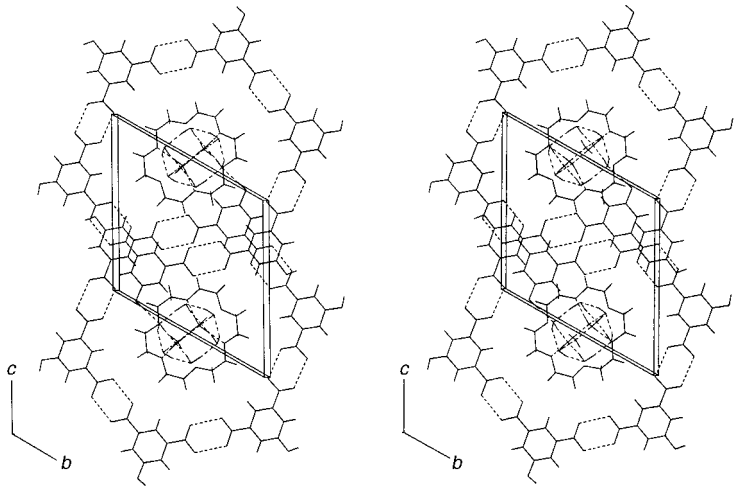

Figure 6. Crystal structure of $(HIPA)_6 \cdot CRO \cdot (H_2O)_{10}$. Stereo line diagram of two neighboring CRO-filled $(HIPA)_6$ honeycomb cages and two associated $(H_2O)_{10}$ clusters. The H bonds are dashed and the cell edges outlined. The view is approximately along the crystallographic *a* axis and perpendicular to the mean plane of the honeycomb cages; compare also Figure 11.

0947-6539/01/0722-4968 $ 17.50+.50/0 *Chem. Eur. J.* **2001**, *7*, No. 22

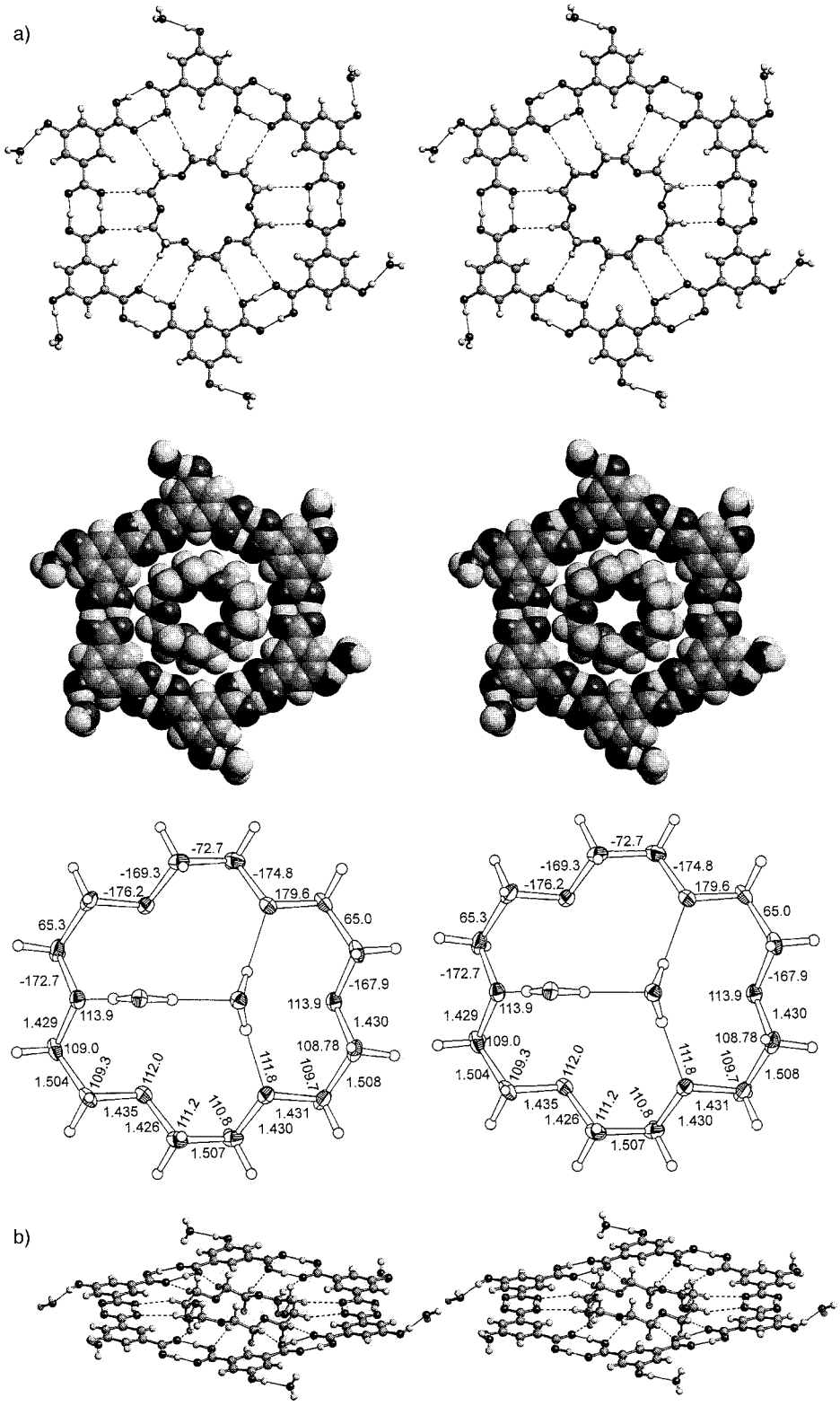

Figure 7. Crystal structure of $(HIPA)_6 \cdot CRO \cdot (H_2O)_{10}$. a) Top: Ball-and-stick and space-filling stereoviews of a $(HIPA)_6$ honeycomb cage accommodating a CRO molecule. Six water molecules belonging to six different $(H_2O)_{10}$ clusters and H-bonded by the phenolic OH groups of HIPA are also shown; O(H)O bonds drawn as thin lines, C–H···O contacts dashed. Below: Identically oriented CRO molecule along with two H-bonded water molecules and geometry data measured at 100 K (bond lengths, bond angles, torsion angles; estimated average standard deviations about 0.001 Å and 0.1°, respectively). The small but significant elliptical distortion of the crown conformation of CRO caused by the hydration is perceptible. b) Oblique side view of a honeycomb cage in order to demonstrate the undulating HIPA molecules, the carboxylic linkages of which "follow" to some extent the equatorial C–H bonds of the CRO molecule suspended in the void, leading to improved C–H···O contacts.

Of course, this holds likewise for the chair form of cyclohexane (Figure 2). The oblique side view of a CRO- filled $(HIPA)_6$ honeycomb cage as drawn in Figure 7b visualizes these somewhat less than ideal directionalities of the equatorial C–H bonds of CRO in the present context, and moreover shows that the embracing six H-bonded HIPA molecules are not fully coplanar either. Instead they are undulating to a certain visible extent around the central CRO molecule, in order to better "follow" the equatorial C–H bonds and to allow more straight C–H···O contacts between CRO and the HIPA carboxyl groups. The undulation of the HIPA molecules is chiefly brought about by small molecular tilts around an axis running through the phenolic C atom of HIPA and the opposite benzene-ring C atom. The direction of the tilting deformations alternates around the $(HIPA)_6$ macroring placing the H-bonded carboxyl pairs alternately above and below its mean plane. Correspondingly, the pairs of equatorial C–H bonds of CRO in contact with the O atoms of the carboxyl pairs are tilted out of the equatorial plane of CRO in alternating directions (by about 20°; Figure 7b). The equatorial C–H following of the HIPA molecules in $(HIPA)_6 \cdot CRO \cdot (H_2O)_{10}$ may be compared to the (more pronounced) "helix following" of the TMA molecules in $(TMA)_2 \cdot HEL$, which also leads to improved, more straight C–H···O contacts between the helically disposed C–H bonds of HEL and the carboxyl groups of the surrounding six H-bonded TMA molecules.[1]

Decameric water cluster $(H_2O)_{10}$ as observed in $(HIPA)_6 \cdot CRO \cdot (H_2O)_{10}$: The second prominent building block of $(HIPA)_6 \cdot CRO \cdot (H_2O)_{10}$ is the

decameric water cluster$(H_2O)_{10}$. It came in fact as a lovely surprise beyond the original crystal planning at the outset of the present study, and provides an extra asset of this intriguing crystal structure considering the intense current interest in structural and spectroscopic properties of oligomeric water clusters.[6] Of course, this interest is spurred by aspirations to better understand the complex properties of bulk liquid water itself. The present centrosymmetric water cluster $(H_2O)_{10}$ is crystallographically fully ordered and has the connectivity of the carbon skeleton of a bishomocubane with the methylene bridges replacing opposite C–C bonds of cubane (Figure 8). The D_{2h} symmetry of this homocubane system is approximated rather well by the positions of the O atoms of the present $(H_2O)_{10}$ cluster; inclusion of the ordered water H atoms reduces the cluster symmetry to C_i. In the crystal, the $(H_2O)_{10}$ clusters are H-bonded to the ether O atoms of CRO and the phenolic O atoms of HIPA (see below). Within $(H_2O)_{10}$, the water molecules are held together by 14 H bonds. Their O···O distances range from 2.658(2) to 3.148(2) Å at room temperature, with an average value of 2.837 Å. These values shrink to 2.645(1)–2.980(1) Å, average 2.787 Å, at 100 K (Figure 8a). For comparison, the corresponding average distances of hexagonal and cubic ice (I_h, I_c) are 2.762 Å (at 223 K)[7a] and 2.750 Å (at 143 K),[7b] respectively. The (uncorrected) H···O distances of the H bonds in the present $(H_2O)_{10}$ cluster extend from 1.69(2) to 2.51(2) Å, average 1.98 Å, at 298 K, and from 1.76(1) to 2.18(1) Å, average 1.93 Å, at 100 K. The O–H···O angles span values between 137(2) and 178(2)°, average 165°, at 298 K, and between 153(1) and 176(1)°, average 169°, at 100 K. Finally, the refined O–H bond lengths of the water molecules of $(H_2O)_{10}$ are between 0.81(2) and 0.97(2) Å, average 0.88 Å, at 298 K, and between 0.85(1) and 0.91(1) Å, average 0.87 Å at 100 K; the H-O–H angles vary from 104(2) to 111(2)°, average 108°, at 298 K, and from 101(1) to 109(1)°, average 106°, at 100 K. It is conspicuous that the two (centrosymmetrically related)

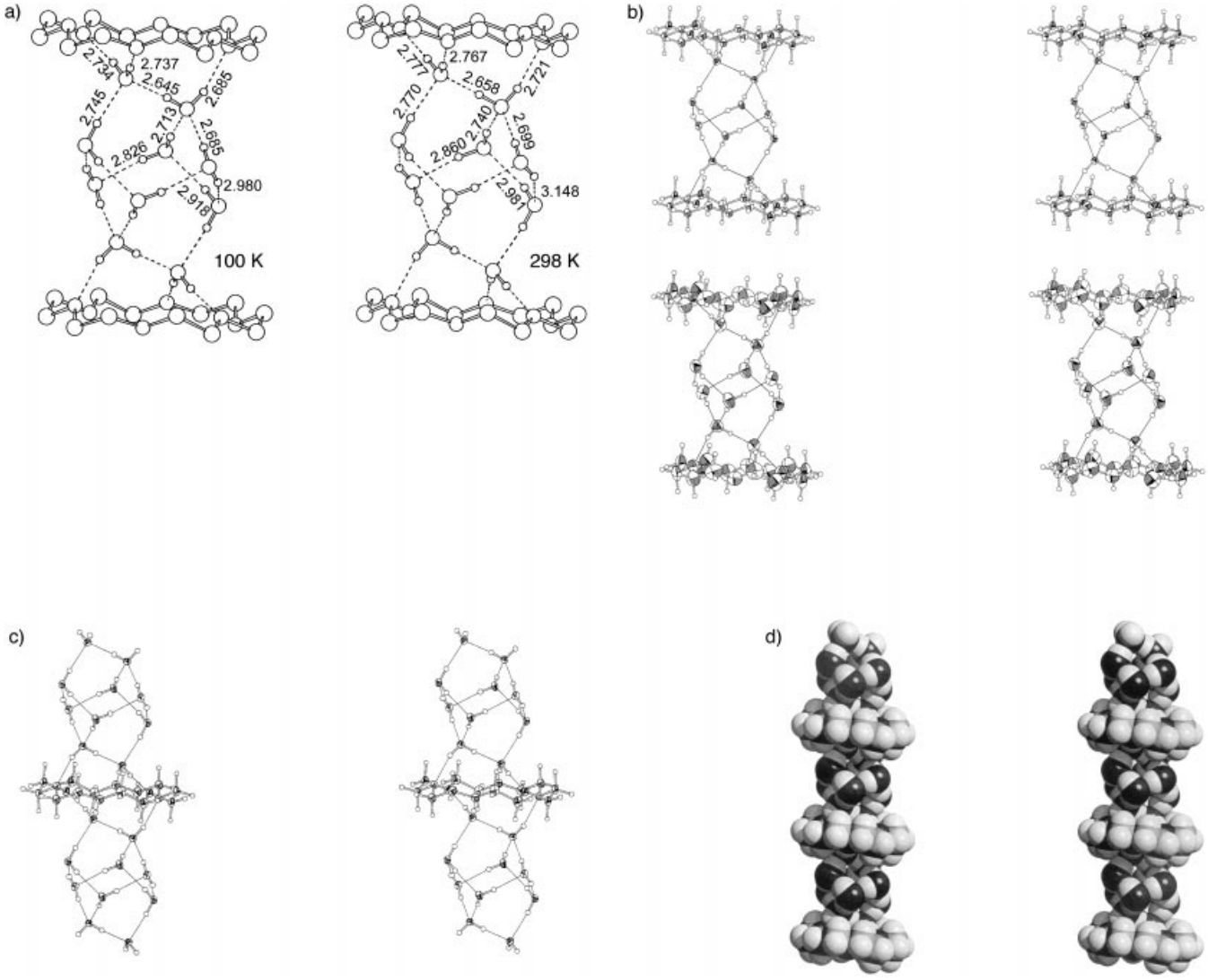

Figure 8. Crystal structure of $(HIPA)_6 \cdot CRO \cdot (H_2O)_{10}$. a) O···O Distances [Å] of the H bonds of the decameric water cluster at 100 K (left) and at 298 K (right); average standard deviations 0.001 and 0.002 Å, respectively. b) Stereoview of a $(H_2O)_{10}$ cluster sandwiched between two H-bonded CRO molecules at 100 K (top) and 298 K (below). 50% Vibrational ellipsoids are shown; in the illustration applying to 100 K, the isotropic temperature factors of the H atoms are divided by a factor of 5, whereas at 298 K spheres of an arbitrary common diameter are drawn for H. Note the more favorable geometry of the longer H bonds at 100 K(see main text). c) Stereoview of a CRO molecule sandwiched by two H-bonded $(H_2O)_{10}$ clusters (100 K). d) Space-filling stereoview of a stack of alternating H-bonded CRO molecules and $(H_2O)_{10}$ clusters. The orientation of the $(H_2O)_{10}$ clusters is essentially the same in all illustrations of this figure.

0947-6539/01/0722-4970 $ 17.50+.50/0 *Chem. Eur. J.* **2001**, *7*, No. 22

relatively long H bonds in $(H_2O)_{10}$ with an O···O separation of 3.148(2) Å at room temperature shrink rather drastically by 0.168 Å to 2.980(1) Å at 100 K, whereas the other O···O separations are on average reduced by only 0.029 Å on cooling (Figure 8a). The two associated long H···O distances are even shortened by 0.33 Å on reducing the temperature, that is from 2.51(2) to 2.18(1) Å. Simultaneously, the O–H···O angle of the two long H bonds becomes substantially more favorable, that is more linear, on cooling (137(2) vs. 153(1)°). The effect is clearly visible qualitatively by comparing the diagrams of Figure 8a, b. A similar observation, but to a lesser extent, applies to the two H bonds the O···O separation of which measures 2.981(2) Å at room temperature: The O···O shortening on cooling is 0.063 Å here with a concomitant increase of the O–H···O angle from 157(2) to 164(1)°. It would thus appear that we are witnessing here the dissociation process of H bonds with increasing temperature, and it should be reassuring to have these findings backed up by a measurement yielding more reliable H positions, that is a variable temperature neutron diffraction experiment. Judging from our experience, growing large crystals of $(HIPA)_6 \cdot CRO \cdot (H_2O)_{10}$ should at any rate not be particularly difficult. It has previously been concluded[6, 8] that at elevated temperatures water clusters with a high degree of connectivity, that is a relatively high number of H bonds per water molecule, are disfavored with respect to those involving smaller numbers of closed H-bonded rings, due to lesser entropy (flexibility) and poorer H-bond cooperativity. An example is provided by $(H_2O)_8$, the monocyclic eight-membered ring form of which dominates in water over the pentacyclic cube-shaped form despite the 50% higher number of H bonds in the latter (12 vs. 8; but note the higher strain of the cube). The observed exceptionally large lengthening at room temperature of some of the H bonds of the present $(H_2O)_{10}$ cluster appears to be in line with these conjectures. Finally, it is noted that aside from other obvious reasons the observation of the pair of long H bonds in $(H_2O)_{10}$ at room temperature had prompted us to perform the low-temperature X-ray measurement (see above).

The most intriguing aspect related to the uncovering of the decameric water cluster in $(HIPA)_6 \cdot CRO \cdot (H_2O)_{10}$ arises from the recognition that its connectivity agrees with that deduced recently from a comparison of vibrational–spectroscopic measurements in the OH stretching range of gaseous $(H_2O)_{10}$ and empirical potential energy calculations.[9] Judging from Figure 4 of reference [9], also the calculated structural details of the oxygen skeleton of the bishomocubane-like $(H_2O)_{10}$ cluster appear to agree rather well with those observed in the crystals of $(HIPA)_6 \cdot CRO \cdot (H_2O)_{10}$. However, the distribution of the O–H bonds among the individual H bonds of $(H_2O)_{10}$ is different in the two models, that is the assignment of the H atoms in the H bonds to the constituting water molecules is not the same. In turn, this difference also leads to a deviating distribution of the H atoms not involved in H bonding in both models. The reason for this difference most likely stems from the fact that the spectroscopic structural model of $(H_2O)_{10}$ (symmetry C_2) corresponds to the free gaseous cluster, whereas our crystal model (symmetry C_i) does not apply to isolated $(H_2O)_{10}$, but rather to a species further H-bonded to CRO and HIPA. Thus, in contradistinction to the spectroscopic model, the $(H_2O)_{10}$ structure in the crystal has to meet the necessities for effective H-bonding to its molecular partners requiring a different distribution of the O–H bonds in the cluster (see below). Structural calculations on the crystal model of $(H_2O)_{10}$ as well as vibrational measurements on crystalline $(HIPA)_6 \cdot CRO \cdot (H_2O)_{10}$ would be of interest. The complex H-bonding pattern of the adduct as a whole may, however, be expected to complicate vibrational analyses considerably. Furthermore, mention is made of another $(H_2O)_{10}$ cluster encountered in the crystals of a hydrated copper complex.[10] In this case the cluster possesses adamantane-like connectivity and is thus held together by 12 H bonds. However, since two opposite O atoms are directly coordinated to copper ions, its connexion with free $(H_2O)_{10}$ appears limited.

The bishomocubane-like decameric water cluster in $(HIPA)_6 \cdot CRO \cdot (H_2O)_{10}$ is held together by 14 H bonds which leaves six O–H bonds available for further H bonding. This holds likewise for six lone pairs on the O atoms of the decamer, which are not engaged in H bonding inside the cluster. The present water decamer is thus capable of maximally donating and and accepting each six H atoms within 12 H bonds towards suitable molecular partners. This H-bonding potential of the $(H_2O)_{10}$ cluster is fully utilized in the crystals of $(HIPA)_6 \cdot CRO \cdot (H_2O)_{10}$. The free "dangling" H atoms in the bishomocubane-like $(H_2O)_{10}$ cluster are grouped three by three at opposite "poles" of the water cage comprising two H_2O molecules each, and are donated to six H bonds towards three ether O atoms each of two CRO molecules. Thus the water clusters are sandwiched between CRO molecules (Figure 8a,b), and in turn the CRO molecules are sandwiched between water clusters (Figure 8c) such that finally H-bonded stacks of alternating CRO molecules and water clusters result (Figure 8d). The O···O distances of the H bonds involving the crown ether O atoms measure 2.685(1), 2.734(1), and 2.737(1) Å at 100 K. The six oxygen lone pairs not engaged in H bonding within $(H_2O)_{10}$ are grouped around a central belt of six O atoms forming a chairlike six-membered ring, and function as acceptors of six H bonds the H atoms of which are donated by the phenolic OH groups of six HIPA molecules (Figure 9). The O···O separations of these phenolic H bonds assume the individual

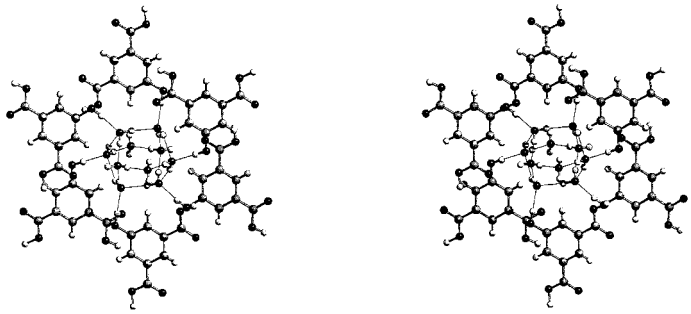

Figure 9. Crystal structure of $(HIPA)_6 \cdot CRO \cdot (H_2O)_{10}$. Stereoview of the distorted octahedral H-bonding of a $(H_2O)_{10}$ cluster by phenolic OH groups of six different $(HIPA)_6$ honeycomb cages as represented solely by the directly bonding HIPA molecules.

independent values of 2.746(1), 2.747(1), and 2.749(1) Å (100 K), and thus agree within experimental error.

The water molecules of the decameric clusters in $(HIPA)_6 \cdot CRO \cdot (H_2O)_{10}$ are thus finally seen to be all tetracoordinated by O(H)O hydrogen bonds. The 10 H_2O molecules of the individual clusters are engaged in a system of altogether 26 H bonds involving 22 O atoms. The average O···O distance of all these H bonds with participation of water molecules amounts to 2.762 Å at 100 K and 2.800 Å at 298 K, respectively, which is close to the corresponding distances found in ice. Rather than grouping the water molecules of $(HIPA)_6 \cdot CRO \cdot (H_2O)_{10}$ in clusters of 10 members, the four of them extending H bonds to CRO may be assigned to these very CRO molecules, corresponding to a formulation $(HIPA)_6 \cdot [CRO \cdot (H_2O)_4] \cdot (H_2O)_6$. Viewed this way, the H-bonded O atoms of the $(H_2O)_6$ entities may be seen to form a chairlike six-membered ring further H-bonded by the phenolic OH groups of six HIPA molecules, and the $CRO \cdot (H_2O)_4$ units correspond to tetrahydrated CRO molecules structurally very similar to those found in $(CHTA)_2 \cdot CRO \cdot (H_2O)_5$ (see above; compare Figure 8 and Figure 4a). The hydration of CRO is likely to be responsible for the observed significant deviations of its crown conformation from D_{3d} symmetry. Closer inspection of Figure 7a shows that the 18-membered ring of CRO is somewhat elliptically distorted with the respective elongation extending horizontally in the diagrams. Apparently the water molecules donating both their H atoms to two H bonds towards ether O atoms of CRO pull together the upper and lower half of the ring perimeter, which leads to somewhat stretched C–H···O contacts between CRO and HIPA in the corresponding sections of the $(HIPA)_6$ honeycomb cage. The space-filling drawing of Figure 7a nicely illustrates this observation. We do not go into quantitative details of this subtle "clamp effect"; suffice it to say that it essentially leads to a symmetry reduction of the CRO ring from D_{3d} to C_{2h}, with the latter symmetry well approximated beyond the crystallographic centrosymmetry. The geometrical data collected in Figure 7a attest to this finding in detail. It should be noted finally that splitting up the decameric water clusters into six-ring-shaped $(H_2O)_6$ units and two opposite pairs of water molecules coordinating to CRO is not by any chance justified by a concomitant splitting of the H-bond lengths. Inspection of the numerical data of Figure 8a shows rather the opposite to be true, in that the O···O distances in these $(H_2O)_6$ chair rings are longest.

Three-dimensional assembly of the molecular building blocks of $(HIPA)_6 \cdot CRO \cdot (H_2O)_{10}$: Let us now turn to the actual three-dimensional crystal structure of $(HIPA)_6 \cdot CRO \cdot (H_2O)_{10}$, that is the assembly of the CRO-filled HIPA honeycomb cages and the decameric water clusters in space. Both building blocks, whose molar ratio is 1:1, are joined in the crystal by H bonds extending from the phenolic OH groups of HIPA to the O atoms of the central $(H_2O)_6$ chair rings as characterized above. The phenolic OH groups function as H donors, and the water lone pairs not engaged in cluster bonding as acceptors. Thus from both the honeycomb cages and the water clusters each six H bonds of this type radiate. The directionality of these sets of six H bonds is distorted octahedral for both types of building block. The distortion from octahedral disposition corresponds to a very severe trigonal compression with approximate coordination symmetry S_6. Each honeycomb cage is singly H-bonded to six decameric water clusters in compressed octahedral fashion, and vice versa each $(H_2O)_{10}$ cluster is analogously H bonded to six honeycomb cages. This is illustrated in Figure 7b and Figure 9; note the extreme, but as such still perceptible, octahedral compression applying to the H bonds emanating from the honeycomb cages. In essence, we are thus dealing with a three-dimensional six-connected network consisting of supercubes severely squashed along a space-diagonal. The corners of the distorted supercubes are represented alternately by the $(HIPA)_6 \cdot CRO$ honeycomb moieties and the $(H_2O)_{10}$ clusters, and the edges are brought about by the H

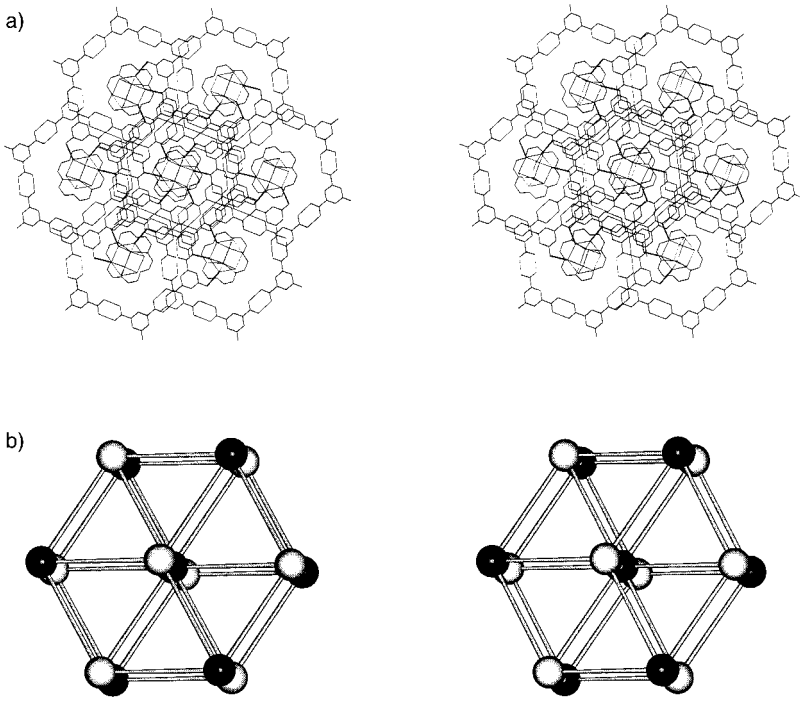

Figure 10. Crystal structure of $(HIPA)_6 \cdot CRO \cdot (H_2O)_{10}$. a) "NaCl aspect" of crystal architecture: Stereoview of two distorted supercubes made up of H-bonded, CRO-filled $(HIPA)_6$ honeycomb cages and $(H_2O)_{10}$ clusters, respectively. The H bonds interlinking these two types of building block in distorted octahedral fashion are drawn as heavier lines. The view is essentially down the approximate trigonal axis of the structure, along which the supercubes are severely compressed; compare with Figure 6 and Figure 11. b) Diagrammatic stereoillustration of the connexion with a trigonally severely compressed NaCl-type architecture. The brighter spheres (e.g. Na^+) represent the CRO-filled $(HIPA)_6$ honeycomb cages, and the darker spheres (e.g. Cl^-) symbolize the $(H_2O)_{10}$ clusters. The interconnecting rods stand for the H bonds extended by the phenolic OH groups of HIPA to the water clusters.

0947-6539/01/0722-4972 $ 17.50+.50/0 *Chem. Eur. J.* **2001**, *7*, No. 22

bonds between the phenolic OH groups and the water molecules of the different building blocks (Figure 10a). The architecture may ultimately be referred to as a severely distorted NaCl-type network, with the CRO-filled honeycomb cages substituting for eaxmple the Na^+ ions, and the water clusters replacing the Cl^- ions (Figure 10b). The H-bond connectivity of the honeycomb cages and water clusters in $(HIPA)_6 \cdot CRO \cdot (H_2O)_{10}$ is similar to the topology of β-hydroquinone (β-HQ), [11a] which builds up two interpenetrating super-octahedral networks in the crystal with trigonally compressed supercubes. The nodes of this three-dimensional network of β-HQ, that is the supercube corners, are established by H-bonded chair rings between six phenolic OH groups, similar to the central H-bonded chair rings of the present $(H_2O)_{10}$ clusters; the supercube edges of β-HQ are represented by the covalent *p*-phenylene units. Since in β-HQ all distorted octahedral nodes are of one type, we are dealing here with a super-polonium rather than a super-NaCl architecture. A single super-polonium HQ network has been found in the adduct $(HQ)_3 \cdot C_{60}$,[11b] the structure of which may thus be regarded even more closely related to $(HIPA)_6 \cdot CRO \cdot (H_2O)_{10}$ than β-HQ itself. The crystal structure of β-HQ is rhombohedral, space group $R\bar{3}$, and a closer analysis of Figure 10a clearly shows that this crystal symmetry is approximated in $(HIPA)_6 \cdot CRO \cdot (H_2O)_{10}$. The deviations from $R\bar{3}$ crystal symmetry in the present case are due to the fact that the $(H_2O)_{10}$ water clusters do not possess trigonal symmetry since their "poles" (see above) consist of only two water molecules H-bonded to CRO. Full threefold symmetry would require a dodecameric water cluster $(H_2O)_{12}$ with six polar water molecules forming H-bonded (strained) three-membered rings in turn H-bonded to CRO. The connectivity of such a water dodecamer would correspond to that of the carbon skeleton of a D_{3d} symmetric heptacyclic hydrocarbon $C_{12}H_{12}$, consisting of a central six-membered cyclohexane chair ring capped on both sides by cyclopropane rings. The lack of $R\bar{3}$ crystal symmetry of $(HIPA)_6 \cdot CRO \cdot (H_2O)_{10}$ may thus ultimately be traced back to the perturbation exerted by the relatively low-symmetric hydration environment of CRO, which causes the reduction to triclinic $P\bar{1}$ crystal symmetry. It is noted that the approximate rhombohedral axes of $(HIPA)_6 \cdot CRO \cdot (H_2O)_{10}$ are defined by the shorter face diagonals of the H-bonded supercubes formed by the $(HIPA)_6 \cdot CRO$ and $(H_2O)_{10}$ building blocks, as discussed above. Figure 10 will help to verify these geometric interrelations, as will the considerations of the following paragraphs, which shall briefly bring us back to this point.

The above description of the crystal structure of $(HIPA)_6 \cdot CRO \cdot (H_2O)_{10}$ as a single three-dimensional six-connected network may be referred to as the "NaCl aspect" of this architecture, highlighted by the formulation $[(HIPA)_6 \cdot CRO][(H_2O)_{10}]$. There is a second convincing possibility to characterize this architecture, which we suggest to refer to as its "host-guest aspect", highlighted by the formulation $[(HIPA)_6][CRO \cdot (H_2O)_{10}]$. Viewed this latter way, the three-dimensional assembly of the $(HIPA)_6$ honeycomb cages is looked upon as a porous host fabric equipped with channels accommodating the guest stacks of H-bonded, alternating CRO molecules and $(H_2O)_{10}$ clusters. The guest stacks are then anchored in the host channels by means of H bonds between the phenolic OH groups of HIPA and the water clusters. On nearer view of Figure 10 it emerges that the $(HIPA)_6$ honeycomb cages may be identified to be arranged in sheets held together by pairs of good C–H···O contacts (across centers of symmetry) between the phenolic O atoms and ortho-positioned aromatic H atoms of two HIPA molecules engaged in neighboring hexagonal cages. A section of such a sheet is shown in Figure 11a, together with enclosed CRO molecules and a $(H_2O)_{10}$ cluster. It may be seen that the phenolic C–H···O contacts make up for the unfavorable circumstance that the phenolic OH groups are engaged in only a single O(H)O bond. The average C···O distance of these C–H···O contacts measures 3.387 Å, which is relatively short. The corresponding average (uncorrected) H···O distance is 2.47 Å, and the associated average C–H···O angle 158° (average refined associated C–H distance, 0.97 Å; all values at 100 K). Figure 11a demonstrates that the sheets formed by the $(HIPA)_6$ units through C–H···O contacts incorporate two kinds of cavities, the larger, by now familiar, hexagonal honeycomb pores, and smaller, more triangular voids lined up by outer edges of three honeycombs. These triangular voids are built from six HIPA molecules held together by alternating pairs of intercarboxylic O(H)O bonds and C–H···O contacts, necessarily three of each. The number of triangular voids is twice that of the hexagonal honeycomb cavities. The sheets of C–H···O-bonded $(HIPA)_6$ honeycomb units are stacked in such a way that the triangular and hexagonal cavities are placed on top of each other, producing channels perpendicular to the sheets. In order to satisfy the 2:1 ratio of the voids, a pair of triangular cavities alternates with one hexagonal pore in the channels. The stacking sequence of the sheets altogether follows the pattern ABCABC···, analogous to that of cubic close-packed spheres and in accord with the above description of the crystal architecture of $(HIPA)_6 \cdot CRO \cdot (H_2O)_{10}$ as a trigonally compressed NaCl-type packing (see also below). The channels thus defined by the stacked $(HIPA)_6$ units are hence seen to be equipped with alternating waists and bulges provided by the triangular and hexagonal cavities, respectively, in the sheets. Accordingly, the $(H_2O)_{10}$ guest clusters are accommodated in the triangular waists and the CRO guest molecules in the hexagonal bulges of the host channels, corresponding to the smaller diameter but larger elongation of the water decamers as compared to the crown conformation of CRO (Figure 11a). As noted above, the alternating $(H_2O)_{10}$ clusters and CRO molecules are interlinked by additional O(H)O bonds leading ultimately to H-bonded guest stacks (Figure 8d), which are anchored in the host channels by means of O(H)O bonds between the outer phenolic OH groups of the $(HIPA)_6$ honeycomb macro-rings and the central H_2O molecules of the water decamers. It so happens that the combined thickness of a $(H_2O)_{10}$ cluster and an H-bonded CRO molecule, that is the thickness of a CRO-$(H_2O)_{10}$-CRO sandwich as shown in Figure 8b, just matches the separation of three stacked sheets of C–H···O-bonded $(HIPA)_6$ hexagons. The thickness of this sandwich is equal to the cell constant a (see below) measuring 10.2371(3) Å at 298 K and 10.0250(3) Å at 100 K (Table 1). This leads to average

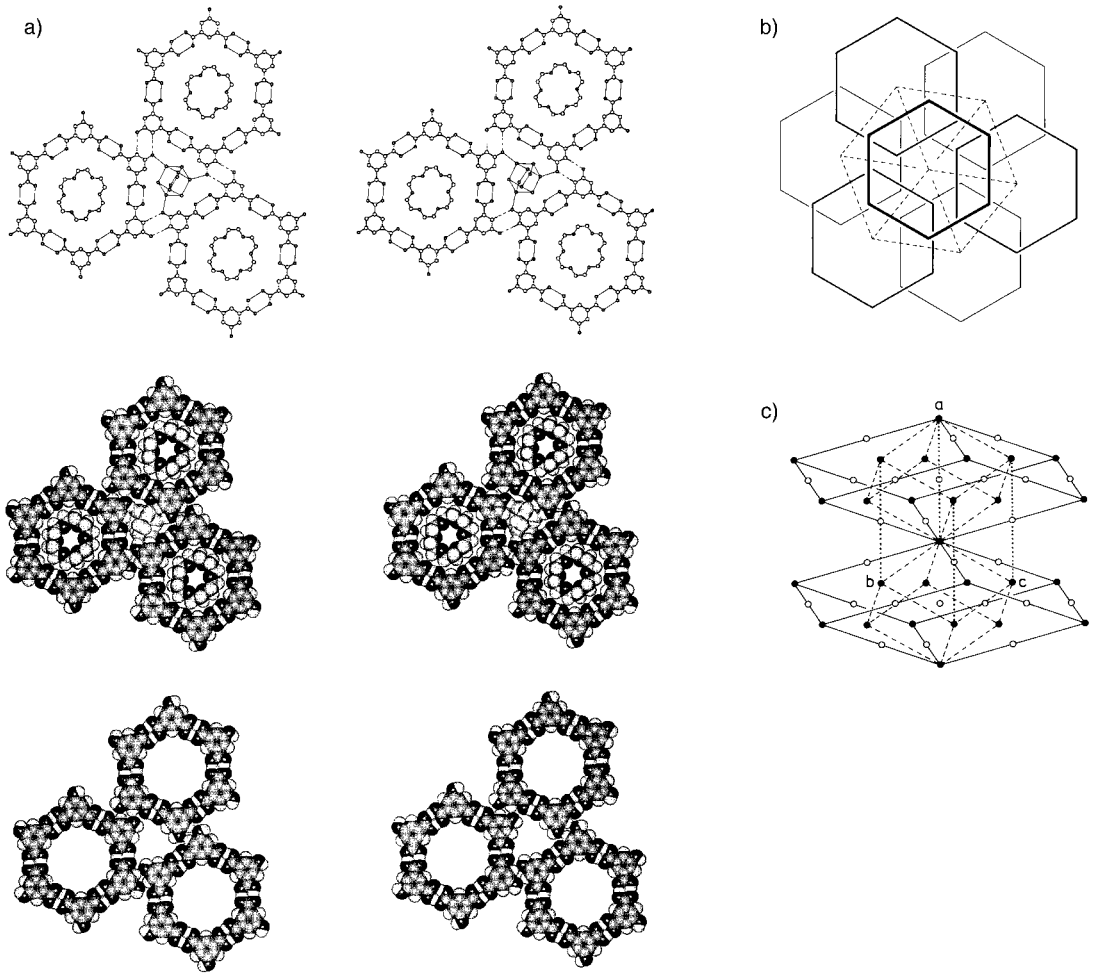

Figure 11. Crystal structure of $(HIPA)_6 \cdot CRO \cdot (H_2O)_{10}$. a) "Host–guest aspect" of crystal architecture. Top and middle: Ball-and-stick and space-filling stereoviews of a section of a sheet of $(HIPA)_6$ honeycomb host cages assembled through phenolic C–H···O contacts (dashed), together with CRO guest molecules and a $(H_2O)_{10}$ guest cluster, anchored in the hexagonal and triangular host voids, respectively. Bottom: Space-filling view without guest systems in order to highlight the cavity shapes. b) Diagrammatic and idealized illustration of the stacking of these sheets in space goup $R\bar{3}$. Only the $(HIPA)_6$ honeycomb cages are drawn and represented as regular hexagons, and the rhombohedral cell edges are outlined (dashed). The sheet sequence is ABCABC... c) All-face-centered distorted cubic, (approximately) rhombohedral, and triclinic choices of the unit cell (full, dashed, and dotted lines, respectively), demonstrating the connection of the NaCl and host–guest aspect, respectively, of the crystal architecture. The representation is diagrammatic and the true trigonal compression is still more pronounced; the cell-edge labels of the triclinic cell are indicated. The full and open circles represent on the one hand CRO-filled $(HIPA)_6$ honeycomb cages and $(H_2O)_{10}$ clusters, respectively, and on the other hand Na^+ and Cl^- ions, respectively.

stacking separations of the $(HIPA)_6$ sheets of 3.412 and 3.342 Å at 298 and 100 K, respectively, perfectly in accord with the usual π-stacking separations of aromatic molecules. The "host–guest aspect" of $(HIPA)_6 \cdot CRO \cdot (H_2O)_{10}$, that is its structural characterization in terms of channel-forming, stacked C–H···O-bonded sheets of $(HIPA)_6$ hexagons, may be related to that of a macrocyclic hexaacetylenic hexaphenol,[12] the topology of which is entirely analogous to that of the H-bonded cyclic hexamer of HIPA. Formally, replacement of the H-bonded carboxyl pairs by covalent acetylenic triple-bond linkages leads directly to the porous hexaphenol, which in the crystal forms O(H)O-bonded sheets stacked very much like the $(HIPA)_6$ hexagons in $(HIPA)_6 \cdot CRO \cdot (H_2O)_{10}$. The hexaphenol molecules are thus also stacked to establish (narrower) channels, which are occupied by solvent guest molecules (methanol and EtOH) H-bonded to the phenolic OH groups protruding into the voids.

Symmetry aspects of the crystal architecture of $(HIPA)_6 \cdot CRO \cdot (H_2O)_{10}$: We conclude our discussion of the crystal structure of $(HIPA)_6 \cdot CRO \cdot (H_2O)_{10}$ with some symmetry considerations uniting the "NaCl aspect" and the "host–guest aspect" of this intriguing solid-state architecture. Figure 11b provides a diagrammatic representation in symmetry-idealized fashion of the stacking pattern of the sheets set up by the C–H···O-bonded $(HIPA)_6$ hexagons. This pattern corresponds to the rhombohedral space group $R\bar{3}$. In actual fact, this crystal symmetry is only approximated by our molecular complex but not strictly obeyed, since the low-symmetric hydration of CRO effects a symmetry reduction to $P\bar{1}$ (see above). In Figure 11b exclusively the $(HIPA)_6$ hexagons are diagrammatically drawn to represent the crystal structure of the adduct, and the guest molecules are omitted in order to bring about the essential symmetry principles of the supramolecular array. Space group $R\bar{3}m$ is precluded by the

0947-6539/01/0722-4974 $ 17.50+.50/0 *Chem. Eur. J.* **2001**, *7*, No. 22

displaced juxtaposition of neighboring corners of the hexagons, representing the corresponding canted C–H···O bonding of the $(HIPA)_6$ honeycomb cages ruling out mirror symmetry. The trigonal and hexagonal sheet cavities as well as the channels defined by their stacking, are readily evident from Figure 11b, as is the stacking sequence ABCABC… of the sheets. The rhombohedral cell edges are also shown in the diagram, thus providing a key to relate the stacked sheets of hexagons to the NaCl structure with the cubic space group $Fm\bar{3}m$. It was pointed out above that the distribution of the CRO-filled $(HIPA)_6$ honeycomb cages and the $(H_2O)_{10}$ clusters is analogous to that of the Na^+ and Cl^- ions in a unit cell severely compressed along a space diagonal (Figure 10). This compression is accompanied by a symmetry reduction from $Fm\bar{3}m$ to the rhombohedral space group $F\bar{3}m$ or $R\bar{3}m$ if one switches to rhombohedral axes, which run from a corner on the trigonal axis of the F-centered unit cell to the three nearest face centers. (Note that the face-centered cubic structure of NaCl may of course also be described in a primitive rhombohedral cell with edges equal to the cubic edges divided by $\sqrt{2}$ and a rhombohedral angle of 60°. By adopting the rhombohedral cell, obviously no full use of the symmetry of NaCl is made, that is the asymmetric structural unit of the primitive rhombohedral cell, space group $R\bar{3}m$, is four times larger than that of the face-centered cubic cell, space group $Fm\bar{3}m$, despite the fourfold volume of the latter.) Removal of the mirror symmetry brings us to space group $R\bar{3}$ as applying to Figure 11b. These geometrical relationships are illustrated in Figure 11c, which in addition shows the triclinic unit cell actually chosen (by the diffractometer software) for our adduct $(HIPA)_6 \cdot CRO \cdot (H_2O)_{10}$. This cell does not correspond to that best approximating the rhombohedral cell since due to the severe trigonal compression, the cell angles of the latter (about 115°) deviate strongly from 90°. The chosen cell is derived from the best (pseudo-) rhombohedral cell through replacing one rhombohedral axis by the shorter space-diagonal parallel to the (approximate) trigonal axis. This leaves one cell angle unchanged while the other two transform to values around roughly 102°. The unchanged pseudo-rhombohedral cell constants are b, c, and α of the Table 1, while the adopted cell edge a corresponds to the shorter space diagonal of the pseudo-rhombohedral triclinic cell. Of course, this is the stacking axis perpendicular to the sheets of the C–H···O-bonded $(HIPA)_6$ honeycomb cages (Figure 6; note shift of origin), and the edge length a is quite naturally seen to represent three times the stacking distance of the sheets, as noted above. The cell angles β and γ of the chosen triclinic cell become equal on approaching rhombohedral symmetry, and then may be shown to be related to α by the equation $2\cos\alpha = 3\cos^2\beta - 1$. It may be verified that in the actual triclinic cell (Table 1) this trigonometric relationship is satisfied to a reasonable degree of approximation. Finally, the stacking sequence ABCABC… of the honeycomb sheets along the a axis also readily follows from the above geometrical and symmetry considerations.

Structure of the molecular complex $(HIPA)_4 \cdot CRO \cdot (EtOH)_2$ with porous distorted HIPA honeycomb double sheets accommodating CRO and EtOH guest molecules: In the course of the crystallizations of the decahydrated 6:1 complex of HIPA and CRO from ethanol (EtOH), some crystals were noticed which appeared to differ from the concurrently grown thick six-sided rods of $(HIPA)_6 \cdot CRO \cdot (H_2O)_{10}$. They took a more compact, polyhedral shape and indeed proved to represent another, different adduct of HIPA and CRO, this time a 4:1 complex containing no water but instead two molecules of EtOH, that is of composition $(HIPA)_4 \cdot CRO \cdot (EtOH)_2$. The X-ray analysis of these likewise triclinic crystals unveiled an intriguing host-guest architecture entirely different from that of the 6:1 decahydrate, but related to the honeycomb sheet structures of $(TMA)_2 \cdot COR$ and $(TMA)_2 \cdot HEL$,[1] which conceptually provided the entry to the present study (see Introduction). We therefore deem it appropriate to round off this report with a description of the crystal structure of the adduct $(HIPA)_4 \cdot CRO \cdot (EtOH)_2$. The adduct $(HIPA)_4 \cdot CRO \cdot (EtOH)_2$ crystallizes in the centrosymmetric triclinic space group $P\bar{1}$ with one formula unit in the unit cell. Accordingly, we are dealing with two symmetry-independent HIPA molecules, one centrosymmetric CRO molecule, and one independent EtOH molecule in the cell. The HIPA molecules of $(HIPA)_4 \cdot CRO \cdot (EtOH)_2$ are assembled in H-bonded, essentially planar sheets with distorted six-sided, honeycomb-type cavities, in which the CRO and EtOH guest molecules are embedded (Figure 12). As in $(TMA)_2 \cdot COR$ and $(TMA)_2 \cdot HEL$, six HIPA molecules participate in the formation of a cavitiy in these two-dimensional three-connected sheets, and are each engaged in three cavities simultaneously. Four of the edges of the distorted honeycomb cavities are provided by pairwise intercarboxylic H-bond linkages between the HIPA molecules, while the remaining two are brought about in opposite position by single O(H)O bonds between the phenolic OH groups. The observed O···O distances of the intercarboxylic H bonds range from 2.628(2) to 2.643(2) Å, average 2.635 Å, and the corresponding interphenolic O···O separation measures 2.693(2) Å. The phenolic linkages are necessarily offset laterally, and the corresponding cavity edges, that is the distance between the benzene-ring centers of the H-bonded HIPA molecules, are shorter than those effected by the intercarboxylic linkages. This leads to cavities, which are smaller in size than the circular voids in $(TMA)_2 \cdot COR$ and $(TMA)_2 \cdot HEL$ brought about entirely by intercarboxylic linkages, and arranges for an elliptic shape of the pores (Figure 13). Quite evidently, the HIPA sheets in $(HIPA)_4 \cdot CRO \cdot (EtOH)_2$ may also be looked upon as being formed by zigzag chains of doubly H-bonded HIPA molecules, which are joined through O(H)O bonds between the laterally protruding phenolic OH groups (Figure 14). Clearly, the assembly of the CHTA molecules of $(CHTA)_2 \cdot CRO \cdot (H_2O)_5$ in distorted honeycomb sheets, as discussed earlier, follows similar topological principles. Here the phenolic linkages of $(HIPA)_4 \cdot CRO \cdot (EtOH)_2$ are replaced by hydrated CRO molecules tying together the lateral carboxylic groups of the CHTA zigzag chains (Figure 4b). Neighboring HIPA sheets in the triclinic crystals of $(HIPA)_4 \cdot CRO \cdot (EtOH)_2$ are related by centers of symmetry, for example those on which the CRO molecules reside. The distorted HIPA honeycomb cavities of the single individual sheets are, however, not strictly centrosymmetric since this

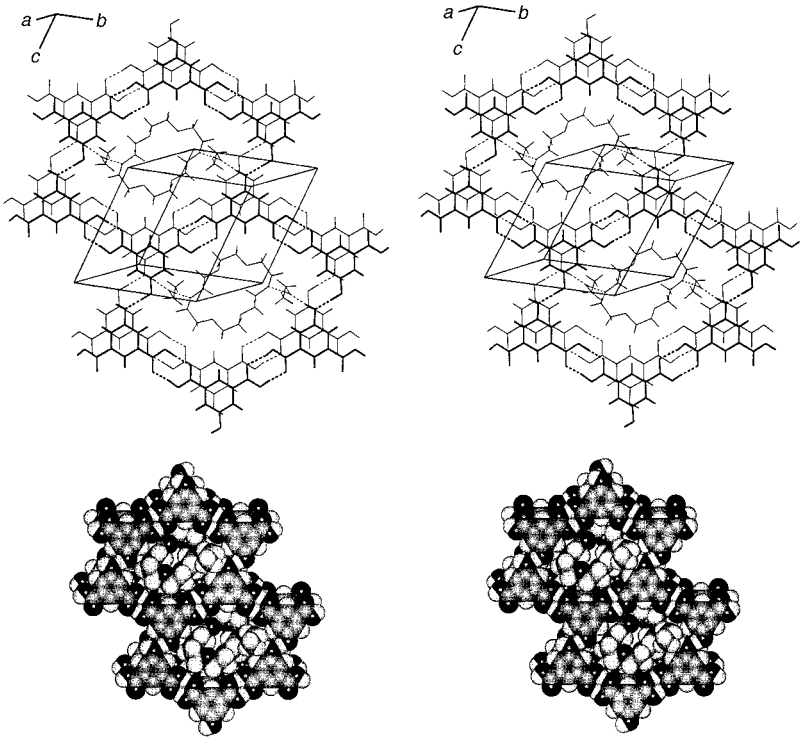

Figure 12. Crystal structure of $(HIPA)_4 \cdot CRO \cdot (EtOH)_2$. Stereo line and space-filling drawings of a section of a HIPA double layer with CRO guest molecules anchored in the two distorted twin honeycomb cavities shown, by means of H bonds through the "assistance" of two interposed EtOH molecules. Cell edges are outlined; only major conformation of CRO drawn.

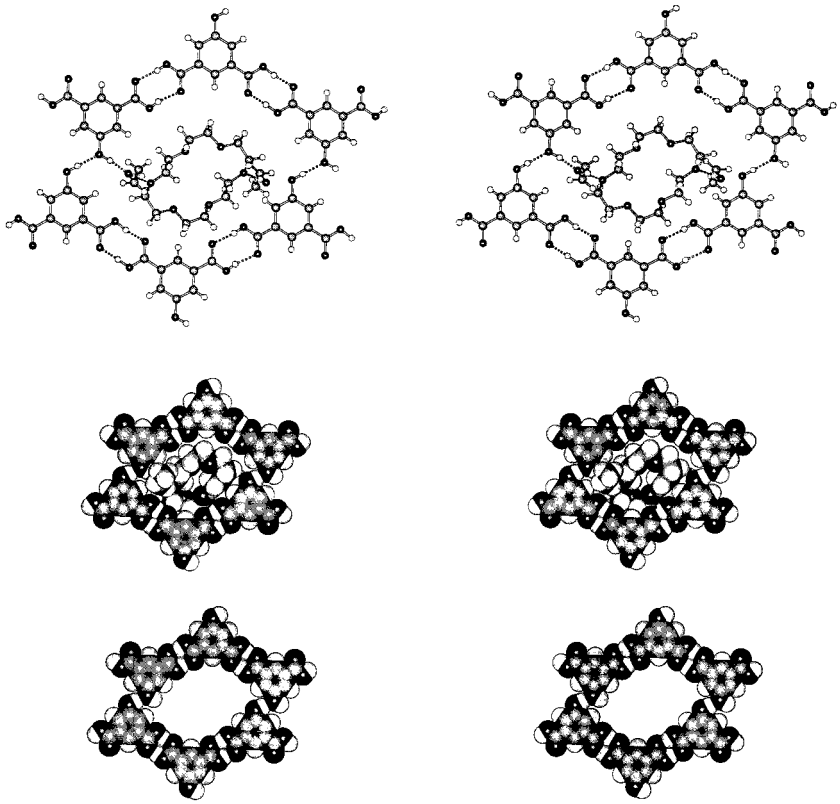

Figure 13. Crystal structure of $(HIPA)_4 \cdot CRO \cdot (EtOH)_2$. Stereo ball-and-stick and space-filling drawings of a single H-bonded, distorted HIPA honeycomb cavity with and without $CRO \cdot (EtOH)_2$ guest units (major CRO conformation drawn only).

does not comply with the phenolic H bonding and the way the CRO and EtOH guest molecules are accommodated in the host voids, as described subsequently.

It is evident from the very concept underlying our present comparative supramolecular analyses that the size of the distorted honeycomb cavities of $(HIPA)_4 \cdot CRO \cdot (EtOH)_2$ cannot be sufficient to accommodate an entire CRO molecule. Moreover, the elliptic shape of the voids is not compatible with the circular crown conformation of CRO. Nevertheless, the stacked, porous three-connected HIPA host sheets altogether do accommodate CRO guest molecules, and the puzzle's solution is that the crown-ether ring extends over two cavities of neighboring sheets, explaining the 4:1 composition of the adduct. Now, the volume of two cavities appears to be larger than that of CRO, such that the guest molecule calls upon the assistance of two EtOH molecules from the crystallization solvent to fill space effectively (Figure 12). The EtOH molecules are H-bonded to two opposite ether O atoms of a centrosymmetric CRO molecule, and in turn receive an H bond from phenolic OH groups of two centrosymmetrically related HIPA host molecules assigned to cavities of neighboring sheets ($O \cdots O$ distances of these H bonds, 2.732(3) and 2.558(3) Å, respectively); note that only one half of the phenolic H atoms are involved in the H bonding of the HIPA host sheets, such that one OH group per cavity is left for binding to EtOH. Through the H bonds of the "EtOH bridges" the distorted HIPA honeycomb sheets of $(HIPA)_4 \cdot CRO \cdot (EtOH)_2$ are thus seen to be tied together in pairs, and the crystal architecture as a whole consists of stacked HIPA double layers in the "twin cavities" of which the

  0947-6539/01/0722-4976 $ 17.50+.50/0 *Chem. Eur. J.* **2001**, *7*, No. 22

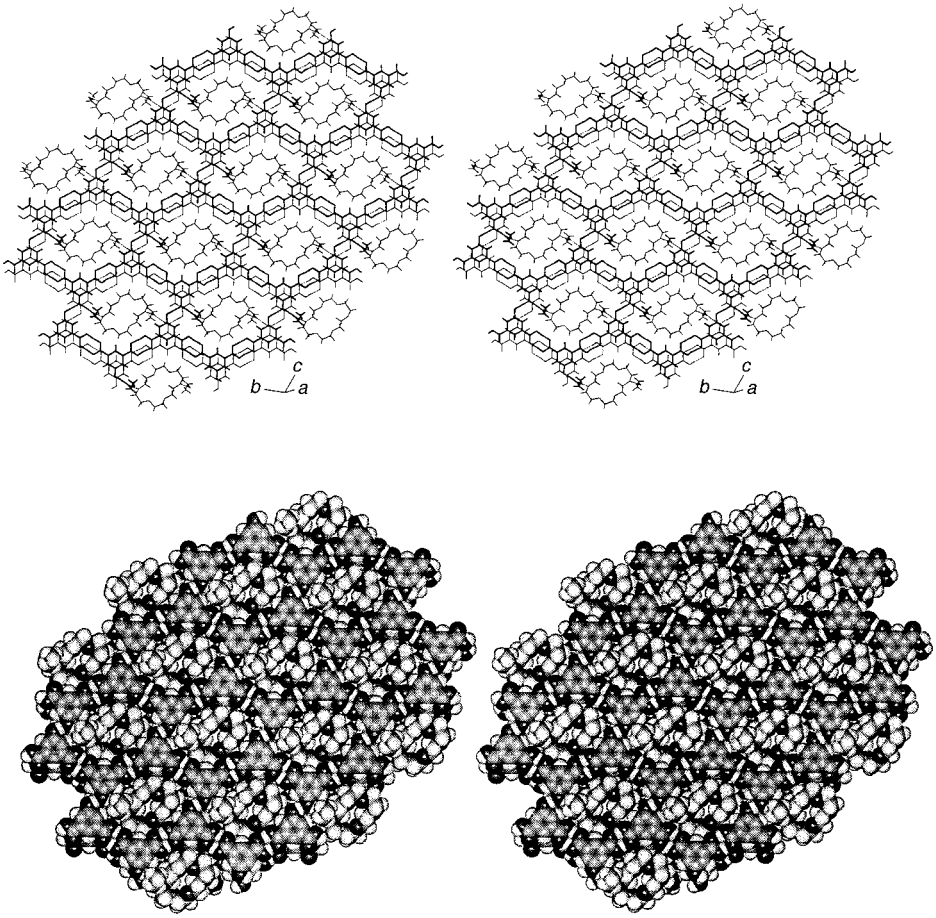

Figure 14. Crystal structure of $(HIPA)_4 \cdot CRO \cdot (EtOH)_2$. Stereo line and space-filling drawings of an extended section of a HIPA host double layer with $CRO \cdot (EtOH)_2$ guest systems suspended in the distorted twin honeycomb host cavities (only major conformation of CRO drawn). Note the HIPA zigzag chains brought about by the standard pairwise intercarboxylic linkages, and tied together through the interphenolic H bonds to complete the distorted honeycomb sheets.

$CRO \cdot (EtOH)_2$ units are suspended. No H bonding occurs between different double layers (Figure 12 and Figure 14). A single cavity of an individual HIPA sheet formally then houses half a CRO molecule and one EtOH molecule. It therefore appears to make sense formulating the adduct as $(HIPA)_2 \cdot CRO_{0.5}$.EtOH, in order to highlight the architectural relationship with $(TMA)_2 \cdot COR$ and $(TMA)_2 \cdot HEL$. As already indicated, the conformation of CRO in the adduct with HIPA and EtOH is not the crown form but rather a leaner, rectangular structure, as detailed further below. However, because of this conformational difference and the fact that the CRO molecules extend over two cavities of neighboring HIPA sheets within a double-layer, and due to the presence of the EtOH molecules, the pattern of C–H···O contacts between CRO and HIPA in the twin voids is much less clear-cut than the respective host-guest contacts in these TMA complexes or in $(HIPA)_6 \cdot CRO \cdot (H_2O)_{10}$.

The H-bonded pairs of distorted HIPA honeycomb host sheets in $(HIPA)_4 \cdot CRO \cdot (EtOH)_2$ are stacked in a laterally displaced fashion such that oblique channels emerge, the axes of which coincide with the cell edge a and are not at right angles with the sheets (Figure 12). The lateral displacement within the pairs of sheets, across the combined cavities of which the $CRO \cdot (EtOH)_2$ guest ensembles extend, is smaller and in another direction than between different such pairs, as may also be concluded from a study of Figure 12. Inside the oblique channels, the H-bonded CRO and EtOH guest molecules are assembled in likewise oblique columns of stacked $CRO \cdot (EtOH)_2$ units, a section of which is shown in Figure 15. Within the guest stacks the $CRO \cdot (EtOH)_2$ units are translationally equivalent along the cell edge a, precisely like the pairs of HIPA sheets accommodating them (Figure 12 and Figure 15). As noted above, the EtOH molecules are H-bonded to both CRO and HIPA and thus mediate the anchoring of the CRO guest molecules in the HIPA host channels. This may be compared to the situation prevailing in $(HIPA)_6 \cdot CRO \cdot (H_2O)_{10}$; here the H bonding of the CRO molecules to the HIPA molecules of the host channels is relayed by the decameric water clusters. Thus in both cases the walls of the HIPA host channels are equipped with protruding phenolic OH groups ready to extend H bonds to suitable acceptor guest molecules.

Conformation of CRO in $(HIPA)_4 \cdot CRO \cdot (EtOH)_2$: It has already been noted that the CRO molecules in $(HIPA)_4 \cdot CRO \cdot (EtOH)_2$ do not adopt the crown conformation, but rather a slimmer, more rectangular form (major conformation; see below) which is better adapted to the roughly elliptic shape of the HIPA host cavities (Figure 16a). This conformation does in fact correspond to that observed in the crystals of CRO itself.[2a] It is noteworthy that only two (centrosymmetrically related) O atoms of CRO are engaged in H bonds in this case, documenting that the rectangular conformation is less in need to alleviate nonbonded repulsions between inner O atoms than the crown conformation. Instead the present rectangular form of CRO is stabilized by two transannular C–H···O contacts. The independent ring torsion angles of the centrosymmetric rectangular CRO conformation as observed in $(HIPA)_4 \cdot CRO \cdot (EtOH)_2$ are as follows (counterclockwise, beginning with the OCCO torsion angle around the lower right CC bond in Figure 16a; values observed in the crystals of CRO itself[2a] in parentheses; standard deviations roughly 0.3 and 0.2°, respectively): −72.2 (−67.6), 179.0(175.5), −173.9 (174.7), 167.0 (174.7), 175.5 (170.1), 78.9 (79.7), −72.0 (−75.4), 167.4 (155.2), −164.7° (−165.8°). The average

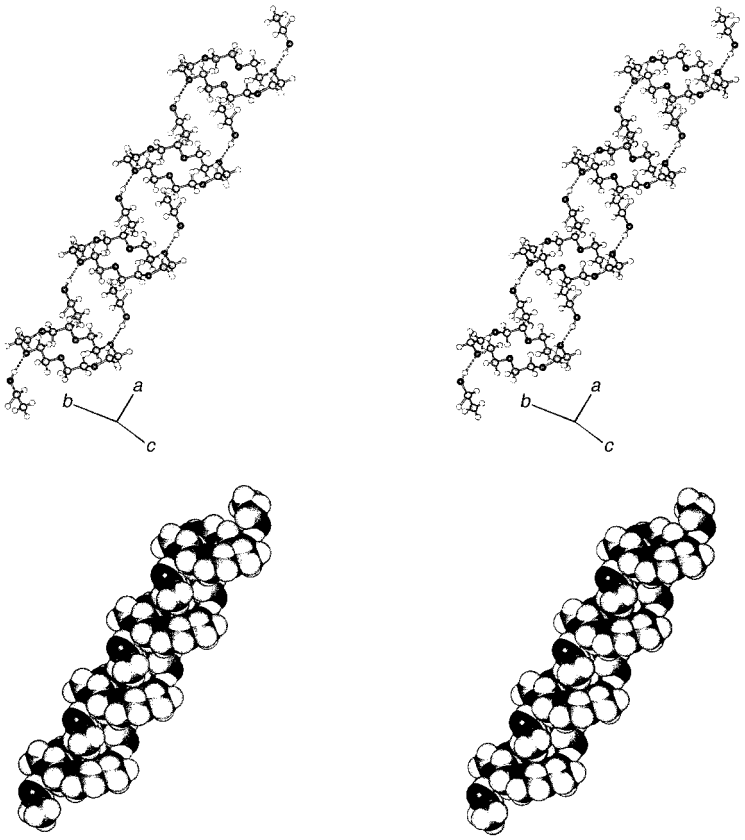

Figure 15. Crystal structure of $(HIPA)_4 \cdot CRO \cdot (EtOH)_2$. Stereo ball-and-stick and space-filling representation of a sequence of $CRO \cdot (EtOH)_2$ guest units, stacked along the crystallographic *a* axis (major CRO conformation drawn only). These guest stacks are anchored in the HIPA host channels through H bonds extended by the phenolic OH groups of HIPA to the O atoms of the EtOH molecules.

absolute deviation of the compared torsion angles is 5.5°, with a maximum difference of 12.2°. No speculation is offered as to the origin of these deviations. In a difference electron density map of $(HIPA)_4 \cdot CRO \cdot (EtOH)_2$ two residual peaks were spotted, located in the area of two opposite (centrosymmetrically related) C–O bonds of the CRO molecule, which were interpreted as indicating a conformational disorder. Proper consideration in the refinements suggested the presence of a minor conformation with a statistical weight of 20%. Correspondingly, the major conformation just described assumed the fourfold weight of 80%. The phenomenon is illustrated in Figure 16a; note that in Figures 12–15 solely the major conformation is drawn. As far as we are aware, the likewise centrosymmetric minor conformation seen in $(HIPA)_4 \cdot CRO \cdot (EtOH)_2$ has not been considered in previous conformational studies of CRO.[2c,d] It is also roughly rectangularly shaped with two transannular C–H···O contacts, and may be related to the crown conformation insofar all O-C-C-O torsion angles are synclinal and their sign alternates. However, whereas the crown conformation of CRO has all 12 C-C-O-C tosion angles close to antiplanar, this holds only for eight of them in the present minor conformation, the remaining four adopting

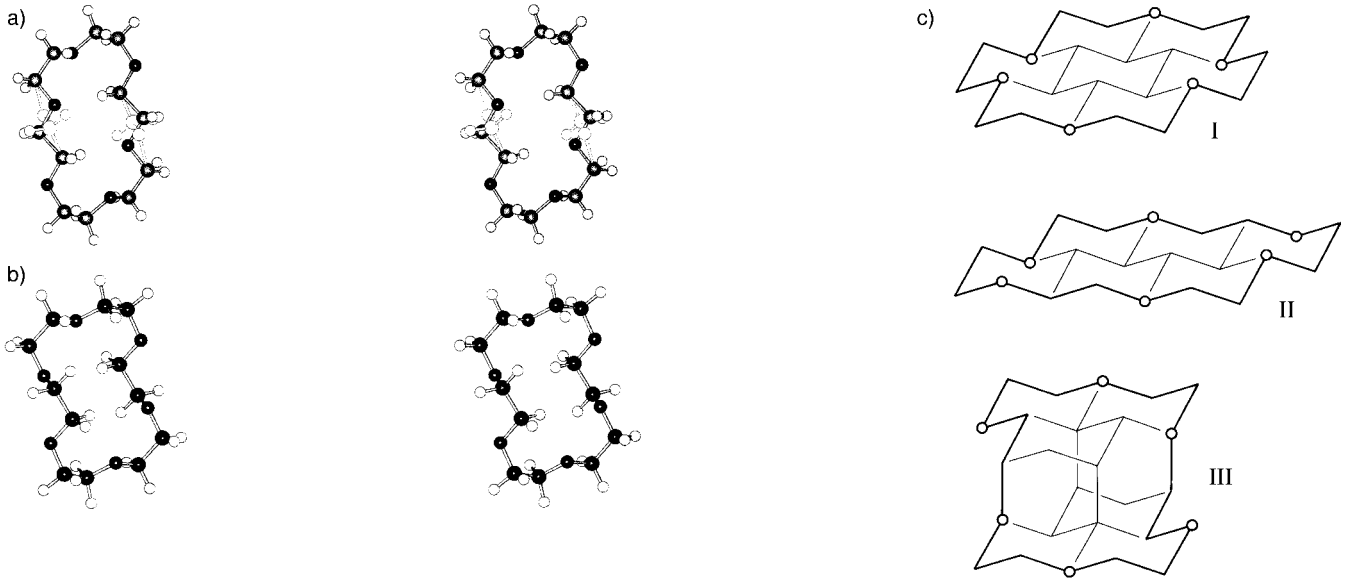

Figure 16. Crystal structure of $(HIPA)_4 \cdot CRO \cdot (EtOH)_2$. Conformational disorder of CRO. a) Stereo ball-and-stick drawing of centrosymmetric major (80%) and minor (20%; open atoms and bonds) rectangular conformations as resulting from a difference electron density map and subsequent refinements. b) Force-field optimized minor conformation. c) The three conformations of CRO encountered in the present study as cut out of the diamond lattice (idealized). **I**: crown conformation; **II**: rectangular conformation occurring in the crystals of CRO itself and in present adduct as major conformation; **III**: new minor conformation in present adduct. The positions of the O atoms are marked by circles.

0947-6539/01/0722-4978 $ 17.50+.50/0 *Chem. Eur. J.* **2001**, *7*, No. 22

synclinal values. An empirical force-field calculation on the new rectangular form of CRO produced an energy minimum about 2.0 kcal mol^{-1} above that calculated for the major conformation as occurring in the crystals of CRO itself. An MM2-type force field without partial charges on the O atoms was used; if reasonable charges are introduced, the minor conformation resulted even more stable than the major conformation. The energy-minimized new centrosymmetric conformation of CRO is depicted in Figure 16b and the calculated independent ring torsion angles are (same sequence as above for major form): -56, -83, 173, 60, 176, 87, -67, -177, -172°. It is noted that the H bonding of the EtOH molecules to CRO in the present adduct with HIPA is little affected by the conformational disorder. The two ether O atoms of CRO involved in the respective H bonds are those pointing away from the ring interior most pronouncedly, and are stereochemically very similar in both conformations (upper right and lower left O atoms in the diagrams of Figure 16; compare also Figure 12). The three conformations of CRO we have encountered in this work, that is the crown conformation (D_{3d} symmetry), the rectangular form as occurring in crystalline CRO and in $(HIPA)_4 \cdot CRO \cdot (EtOH)_2$ as major conformation (C_i), and the minor conformation in this adduct (C_i), are all "diamond conformations",[13] that is their (idealized) C,O ring skeleton may be cut out of the diamond lattice (Figure 16c). The crown conformation of CRO may thus be seen to be superimposable on the perimeter of all-*trans*-perhydrocoronene, while the rectangular crystal form of CRO (major conformation in present adduct with HIPA and EtOH) fits the outer 18-membered ring of all-*trans*-perhydroanthanthrene. The new minor conformation as observed in $(HIPA)_4 \cdot CRO \cdot (EtOH)_2$ is not defined within a single sheet of *trans*-fused cyclohexane chair rings (Figure 16c).

H-Bonding pattern in the crystals of HIPA·$(H_2O)_2$: We conclude the present account with a brief portrayal of the crystal structure of HIPA, which has given us much of the present attractive supramolecular crystal chemistry. With some difficulty, suitable crystals of HIPA could be grown from aqueous EtOH which turned out to correspond to a dihydrate, $HIPA \cdot (H_2O)_2$. The crystals are needle-shaped with rhomb-like cross-section and adopt the space group $P2_1/c$ with four formula units in the unit cell (Table 1). The HIPA and water molecules assemble in gently corrugated sheets with a fairly complex, yet fully ordered H bonding pattern (Figure 17a). The dicarboxylic acid molecules set up meandering chains linked up by single H bonds between the carboxylic groups rather than the usual pairwise H-bond linkages (drawn in bold in Figure 17a; O···O distance 2.657(1) Å). In each U turn of these strongly winding chains a water molecule is embedded, which is H-bonded to a carboxyl CO and a phenolic OH group, respectively, of two neighboring HIPA molecules. These hydrated HIPA chains are then laterally H-bonded with the help of water molecules of another type to complete the sheets. Altogether four different H-bonded ring architectures may be discerned in the sheets, composed of six, eight, and

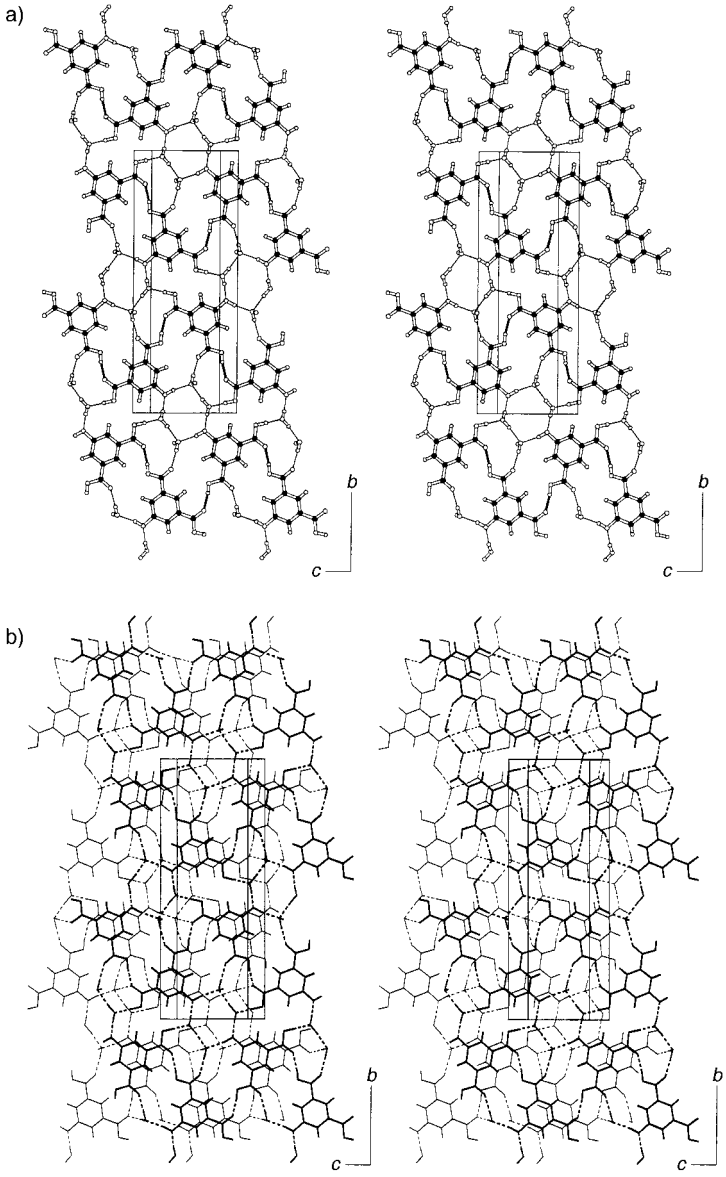

Figure 17. Crystal structure of $HIPA \cdot (H_2O)_2$. Ball-and-stick and line stereo diagrams showing a) one corrugated H-bonded sheet with single intercarboxylic H-bond linkages in bold, and b) two neighboring layers linked up by H bonds between tetracoordinated water molecules and carboxyl CO groups. The H-bonded fabric is altogether three-dimensional.

twice 14 members counting only the constituent C and O atoms. The H-bonded six-membered ring (a chair form) and one of the 14-membered rings are centrosymmetric (Figure 17a). The stacking mode of the H-bonded layers is very simple with the sheet sequence AAA…, corresponding to the elementary translation along the short cell edge $a =$ 3.6740(1) Å (Table 1). The water molecules characterized as sitting in the U turns of the HIPA chains are tetracoordinated and extend a H bond to the carbonyl O atom of a carboxyl group of a HIPA molecule assigned to a neighboring sheet, such that the complete H-bonded network of HIPA · $(H_2O)_2$ ultimately becomes three-dimensional (Figure 17b). According to the fairly high crystal density of 1.562 g cm^{-3} (Table 1), the packing efficiency of this molecular fabric appears good.

Conclusions

The initial stereochemical comparison of the molecular shapes of COR, HEL, and CRO permitted us to accomplish a piece of successful crystal engineering and has led us to interesting supramolecular chemistry of hydrated (EtOH-solvated) complexes between CRO and di- and tricarboxylic acids. In addition, and quite unexpectedly, it presented us with an intriguing decameric water cluster the connectivity of which agrees with that derived from vibrational–spectroscopic gas-phase measurements. Our study once again attests to the high versatility of CRO as a potent vehicle and template in supramolecular applications.[2b] The present results demonstrate the effective stabilization of the crown conformation of CRO by hydration. Furthermore, it emerges that hydrated CRO is a rather avid H-bond acceptor, apparently leading in particular to a high general propensity for binding to carboxylic acids. Accordingly, we have found quite a few further examples of hydrated complexes between CRO and carboxylic acids. Finally, the observation of the water decamer in $(HIPA)_6 \cdot CRO \cdot (H_2O)_{10}$ entertains hope that other interesting water clusters and hydrate architectures might be uncovered in the solid state through studies of further hydrated molecular complexes of CRO with H-bond donors. Related experiments should be straightforward given the ready availability of CRO and its versatile solubility properties.

Experimental Section

Crystallizations and crystal structure analyses: All the required chemicals of the present study are readily available allowing relatively large crystallization batches. The crystallizations, generally from EtOH or aqueous EtOH, that is under ambient (humid) conditions, also benefitted from favorable solubility properties of the molecular components such that large crystals could be grown throughout. The crystallographic X-ray measurements were performed at room temperature on a Nonius four-circle diffractometer equipped with a CCD area counter using Mo radiation ($\lambda = 0.71073$ Å). For $(HIPA)_6 \cdot CRO \cdot (H_2O)_{10}$, in addition a low-temperature measurement was undertaken at 100 K (see main text for details). The crystal structures were solved and refined with the help of the programs SHELXS97 and SHELXL97, respectively. Crystal and X-ray analytical data of the five more prominent molecular complexes of the present work are collected in Table 1 and have been deposited.[14]

[1] O. Ermer, J. Neudörfl, *Helv. Chim. Acta* **2001**, *84*, 1268.

[2] a) J. D. Dunitz, P. Seiler, *Acta Cystallogr. Sect. B* **1974**, *30*, 2739; E. Maverick, P. Seiler, W. B. Schweizer, J. D. Dunitz, *Acta Crystallogr. Sect. B* **1980**, *36*, 615; b) I. Goldberg in *Inclusion Compounds*, *Vol. 2* (Eds.: J. L. Atwood, J. E. D. Davies, D. D. MacNicol), Academic Press, New York, **1984**, p. 261; c) M. J. Bovill, D. J. Chadwick, I. O. Sutherland, D. Watkin, *J. Chem. Soc. Perkin Trans. 2* **1980**, 1529; d) G. Wipff, P. Weiner, P. Kollman, *J. Am. Chem. Soc.* **1982**, *104*, 3249.

[3] E. H. Nordlander, J. H. Burns, *Inorg. Chim. Acta* **1986**, *115*, 31.

[4] R. Alcala, S. Martinez-Carrera, *Acta Crystallogr. Sect. B* **1972**, *28*, 1671.

[5] J. Yang, J.-L. Marendaz, S. J. Geib, A. D. Hamilton, *Tetr. Lett.* **1994**, *35*, 3665; J. R. Fredericks, A. D. Hamilton in *Comprehensive Supramolecular Chemistry*, *Vol. 9* (Eds.: J. L. Atwood, J. E. D. Davies, D. D. MacNicol, F. Vögtle), Pergamon, **1996**, Chap. 16, p. 565.

[6] J. M. Ugalde, I. Alkorta, J. Elguero, *Angew. Chem.* **2000**, *112*, 733; *Angew. Chem. Int. Ed.* **2000**, *39*, 717; R. Ludwig, *Angew. Chem.* **2001**, *113*, 1856; *Angew. Chem. Int. Ed.* **2001**, *40*, 1808.

[7] a) S. W. Peterson, H. A. Levy, *Acta Crystallogr.* **1957**, *10*, 70; b) H. König, *Z. Kristallogr.* **1944**, *105*, 279.

[8] F. Weinhold, *J. Chem. Phys.* **1998**, *109*, 373.

[9] U. Buck, I. Ettischer, M. Melzer, V. Buch, J. Sadlej, *Phys. Rev. Lett.* **1998**, *80*, 2578.

[10] L. J. Barbour, G. W. Orr, J. L. Atwood, *Nature* **1998**, *393*, 671.

[11] a) D. E. Palin, H. M. Powell, *J. Chem. Soc*. **1947**, 208; D. D. MacNicol in *Inclusion Compounds, Vol. 2* (Eds.: J. L. Atwood, J. E. D. Davies, D. D. MacNicol), Academic Press, New York, **1984**, p. 1; b) O. Ermer, *Helv. Chim. Acta* **1991**, *74*, 1339.

[12] D. Venkataraman, S. Lee, J. Zhang, J. S. Moore, *Nature* **1994**, *371*, 591.

[13] M. Saunders, *Tetrahedron* **1967**, *23*, 2105.

[14] Crystallographic data (excluding structure factors) for the structures reported in this paper have been deposited with the Cambridge Crystallographic Data Centre as supplementary publication nos. CCDC-161617–CCDC-161622. Copies of the data can be obtained free of charge on application to CCDC, 12 Union Road, Cambridge CB2 1EZ, UK (fax: (+44) 1223-336-033; e-mail: deposit@ccdc.cam.ac.uk).

Received: June 7, 2001 [F3320]